AN ABSTRACT OF THE THESIS

James Gilbert Pavlovich for the degree of Doctor of Philosophy in Chemistry presented on March 18, 1993.

Title: Ion Pairing of Nucleotides with Surfactants for Enhanced Sensitivity in Liquid Matrix Assisted Secondary Ion Mass Spectrometry

Abstract approved: Redacted for Privacy

Douglas F. Barofsky

In particle induced desorption-ionization mass spectrometry the strength of an analyte's signal under a given set of bombardment conditions is usually considered to be representative of the analytes relative surface activity. This rationale is generally used to explain differences in the technique's sensitivity between and within various classes of compound. In liquid matrix assisted secondary ion mass spectrometry (SIMS) sensitivity enhancement of ionic analytes by pairing with surface active counterions has been demonstrated by several groups. This technique has been utilized in this work to achieve a 10,000 fold enhancement in the signal for ATP on a double focusing magnetic sector instrument and to detect femtomole quantities of nucleoside monophosphates on a time-of-flight instrument. The analyte's signal, however, is dependent on both the analyte bulk concentration and that of the surfactant. Additionally, the surfactant concentration that produces the maximum analyte signal changes with the analyte concentration. In this study, this phenomenon has been modeled in terms of conventional solution equilibria and surface chemical principles. It is assumed that the initial surface composition and the bulk concentration are the boundary conditions of a steady state established by the competing processes of surface sputtering and surface replenishment from the bulk during analysis. Calculated surface excesses correlate well with observed relative ion intensities, suggesting that equilibrium conditions are approached in the sample matrices despite the outwardly dynamic nature of the sputtering processes.

Ion Pairing of Nucleotides with Surfactants for Enhanced Sensitivity in Liquid Matrix Assisted Secondary Ion Mass Spectrometry

by

James Gilbert Pavlovich

A THESIS

submitted to

Oregon State University

in partial fulfillment of
the requirements for the
degree of

Doctor of Philosophy

Completed 18 March 1993

Commencement June 1993

APPROVED:

Redacted for Privacy

Professor of Agricultural Chemistry in charge of major

Redacted for Privacy

Chairman of department of Chemistry

Redacted for Privacy

Dean of Graduate School

Date thesis is presented 18 March 1993

Typed by researcher for James Gilbert Pavlovich

Acknowledgements

I would like to thank Brian Arbogast, Lilo Barofsky, Susan Chen, Judit Kopniczky and Robert Yen for their help in collecting the data presented in this thesis. I also wish to thank John Jones and Armando Herbelin for help with the computer programs used for equilibrium calculations.

I received financial support during this project from Northwest Organization for College and University Science (NORCUS), the United States Department of Energy, the Ford Foundation and the department of Chemistry at Oregon State University.

Finally, I would like to thank my major professor, Douglas Barofsky, for his direction and unfailing support throughout my graduate program.

Table of Contents

List of Figures

Ion Pairing of Nucleotides with Surfactants for Enhanced Sensitivity in Liquid Matrix Assisted Secondary Ion Mass Spectrometry

Chapter 1

Background

1.1.1 Fast Atom Bombardment and Secondary Ion Mass Spectrometry

In 1981, Barber, et al. first demonstrated the use of fast atom bombardment (FAB) as an ion source for mass spectrometric analysis of involatile organic molecules.[1] Two major factors distinguished this work from previously reported particle induced desorption experiments. Where Macfarlane employed MeV fission fragments of ^{252}Cf decay[2] for sample bombardment in plasma desorption mass spectrometry (PDMS) and Benninghoven used a beam of keV Ar^+ ions for so-called static secondary ion mass spectrometry[3] (SIMS), Barber used, as the name implies, a beam of neutral keV atoms to bombard the sample substrate. More significantly, the sample matrix employed by Barber was a drop of liquid glycerol into which analyte molecules had been mixed.

It soon became apparent, in the instance of FAB, that the nature of the primary particle was of lesser importance than the nature of the matrix. Indeed, it was demonstrated that a primary ion beam produced virtually the same spectrum as one composed of neutral atoms.[4] Ion beams have advantages over neutral particle beams in certain applications where it is desirable to focus or deflect the beam.[5] For this

reason the use of primary ions to desorb ions from liquid matrices has come into widespread use and is termed dynamic or liquid matrix assisted SIMS or liquid SIMS (LSIMS) for short. In this thesis, the term LSIMS will be employed to describe the analysis of secondary ions produced by sputtering from liquid matrices regardless of the charge state of the primary particle used.

1.1.2 The Role of the Liquid Matrix

The primary advantage of liquid matrices is that their use vastly extended the range of molecules, both in terms of class and size, that are amenable to accurate mass analysis. Additionally, the dynamic nature of the liquid matrices significantly increases the time scale over which spectra could be obtained. In the cases of PDMS and static SIMS, a monolayer or submonolayer of analyte was adsorbed onto the solid substrate. The current densities of the primary particles are necessarily low ($< 10^{-8}$ A/cm^2) in order to limit the collision induced damage to organic molecules on the surface due to particle bombardment. A considerable area of damage is left by each incident particle due either to direct collision of the incoming particle with a molecule on the surface or excitation induced decomposition by energy deposited indirectly by the incident particle to the substrate. Particles impinging on a damaged area of the surface will generally yield no useful ions and may contribute background in the form of chemical debris. Low current densities minimize the probability of two particles striking the same area of the surface in the time needed to obtain a spectrum. The liquid matrix provides a

means of renewing the target surface through diffusion from the bulk solution or by convection accompanying bombardment. Additionally, products of beam induced damage need not remain at the surface. For these reasons, even when using primary ion current densities on the order of 10^{-6} A/cm^2, spectra are routinely obtained from liquid matrices over time frames of tens of minutes or more without significant effects from beam induced sample damage.

Although glycerol is by far the most popular matrix in use for LSIMS analysis, a number of other compounds have been demonstrated to provide satisfactory and even superior results for specific classes of analytes.[6] To date, searches for such matrices have been largely empirical in nature as the mechanisms of ionization from liquid matrices are not well defined. Recently, in an attempt to facilitate fundamental studies toward a more rational approach to experimental design, Cook et al. have compiled a list of physical and chemical properties for a number of common LSIMS matrices.[7] A few general properties have emerged as requirements for useful matrices.

Low volatility is essential in order to maintain a liquid state under the vacuum conditions of the ionization source (typically 10^{-7} to 10^{-5} torr). It is generally observed that secondary ion emission ceases when the matrix evaporates despite the fact that the analyte is typically of significantly lower volatility and therefore still present on the target.[8] Solvation is apparently necessary in order to insure ionization. Secondary ion currents are generally observed to be stronger and more prolonged when

the sample is actually dissolved in the matrix in opposition to being presented as a suspension or mull. Solution chemistry can be manipulated to increase the efficiency of ion desorption as will be demonstrated by the experiment presented in this thesis.

Mass transport of analytes from the bulk to the surface is related to the viscosity of the matrix.[9] When the surface composition differs significantly from that of the bulk this effect is enhanced. Once the initial surface is sputtered away, the secondary ion current would presumably reach a steady state that is mass-transport limited. If the time frame for exhausting the surface is significantly less than that for refreshment, one would expect the secondary ion signal to be more representative of the bulk composition than that of the undisturbed surface. This phenomenon will be discussed in greater detail in a later section. A second consideration in regard to the viscosity of the matrix is the physical orientation of the sample plane in the instrument. If the target is not horizontal, sample "drooping" will occur to a greater extent with lower viscosity matrices.

Ideally the matrix should be chemically inert toward the analyte. In practice, however, reactions often occur, particularly under the energetic conditions of particle bombardment. Specific examples reported in the literature include ligand exchange reactions.[10] esterification of acidic analytes,[11,12] and reduction of compounds containing low lying unoccupied molecular orbitals.[13,14] In addition to complicating spectral interpretation, matrix-analyte reactions can be detrimental with regard to sensitivity

when ionization of the sample is incomplete or results in more than one reaction product.

Finally, as the matrix is subjected to desorption/ionization as well as the analyte, one must consider the contributions of the matrix to the mass spectrum. Field has studied and discussed in detail the mass spectrum of glycerol in terms of the radiation chemistry and the resulting fragment ions.[15] The predominant ions formed from glycerol under particle bombardment include the molecular ions, $(G+H)^+$ and $(G-H)^-$ where G is the glycerol molecule, in positive and negative ion analysis modes, respectively. Additionally, association clusters can be observed with the formula $(G_n+H)^+$ where n = 1, 2, 3 .... Such clusters with as many as fifteen glycerol molecules have been observed. In negative ion mode an analogous series of $(G_n-H)^-$ ions can be observed. Significant fragment ions include those corresponding to the neutral losses of one and two waters from the molecular ion and the neutral loss of methanol from the molecular ion. Other fragment ions are observed at m/z 45, 43, 31, and 29 in positive ion mode and m/z 71,45,43, and 41 in negative ion mode. Typical spectra for glycerol in each analysis mode are shown in figure 1.1. Field also notes that additional ion peaks may appear as bombardment proceeds due to formation of new products as a result of radiation damage. With some analytes solvation clusters of the formula $(M+G_n+H)^+$ or $(M+G_n-H)^-$, where M is the analyte molecule, are observed. Each matrix will, of course, have its own distinct mass spectrum, and matrix choice takes into account the possibility of spectral interferences. Larger analytes are less

Figure 1.1. LSIMS spectra of glycerol in a) positive and b) negative ion detection modes.

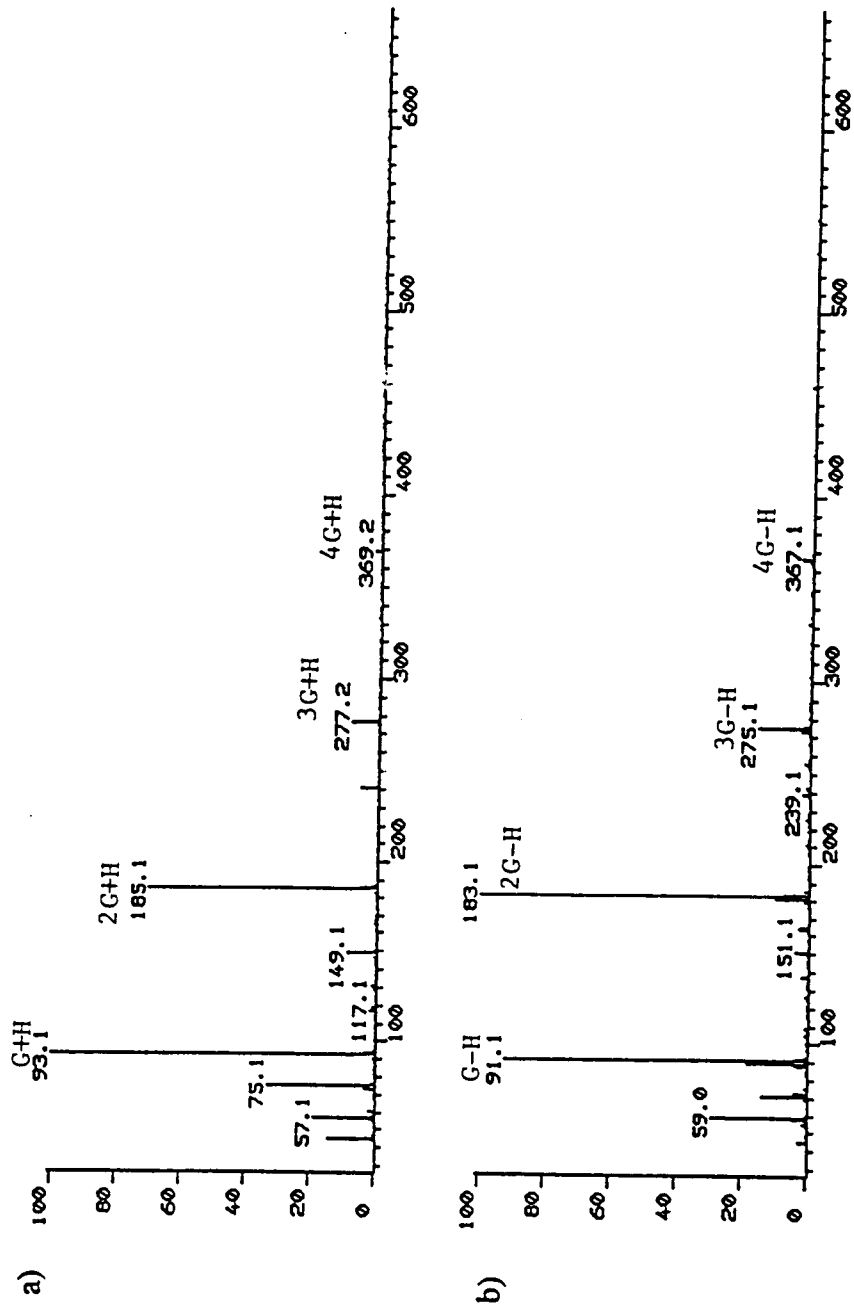

subject to such interferences since most matrices are on the order of 100 to 200 amu in molecular weight and present relatively few ion peaks above the molecular weight.

1.1.3 Physical Aspects of Sputtering

The present study is primarily concerned with the chemical aspects of liquid matrix assisted SIMS. However, a general familiarity with the physical mechanisms governing particle desorption is necessary in order to establish a context in which to discuss the observed chemistry. Fundamentally, the kinetic energy of the primary particle is transferred to particles in the target medium. As a consequence, secondary particles are emitted from the surface of the energized volume.

It is useful to employ a parameter called the stopping power (dE/dx) defined as the rate at which the energy of the primary particle is deposited to the target medium per unit of distance travelled by the primary particle through that medium. Energy is transferred from primary particle to target as a result of two distinct processes: elastic nuclear collisions and electronic excitation.[16,17,18] For particles possessing energies in the low keV range, the dominant process of energy transfer is that of elastic collisions between the nuclei of incoming and target particles. This is termed nuclear stopping. The interactive force is purely coulombic in nature, and the stopping power can, therefore, be calculated from the particle masses and atomic numbers and the initial energy of the incoming particle. In such a process the incoming particle directly

imparts momentum to the target particles with which it collides. In electronic stopping the primary particle interacts with the electron cloud of the target particles. The kinetic energy of the primary particle is transferred via the generation of electron-hole pairs in the target material. Conversion of this electronic excitation to kinetic energy of the target particles must then occur through a second mechanism. Electronic stopping becomes an important process for primary particles whose energies are in the high keV to MeV range. The primary particle energies used in the current study are generally less than 10 keV. In this realm the dominant energy transfer process is through elastic scattering. At these energies the coulombic force experienced by the colliding particles is somewhat screened and this must be taken into account when calculating stopping powers.

1.1.4 Atomic Collision Cascades and Thermal Spikes

Sigmund developed the theory of atomic collision cascades most widely used to describe sputtering from the surface of a conducting target in an atomic SIMS experiment.[19] In a linear cascade the deposition of energy occurs through a series of elastic collisions between primary and target particles as the primary particle travels through the target medium. With each collision the primary particle gives up some of its kinetic energy to its collision partner. The target particle, now possessed of that kinetic energy, may strike other particles and further distribute the energy. Statistically, some of the particles set in motion in this manner will acquire momentum

in the direction of the target surface. Those particles reaching the surface may escape into the gas phase if they possess sufficient energy to overcome the surface binding forces. The fundamental assumption in this model is that the rate of energy deposition is so low that each collision can be treated as an individual binary event that follows the Boltzmann transport equation. In this model, a relatively small fraction of matrix particles are ultimately set in motion by the incident particle. Using transport theory, Sigmund developed a general equation for sputtering yield:

$$Y = \Lambda F_D, \qquad (1\text{-}1)$$

where Λ is a material parameter and F_D, a complex function of mass ratio, M_1/M_2, incident angle, θ, and initial energy, E_0, of the primary ion, is the stopping power at the surface of the target. It must be noted that the atomic collision cascade theory was developed for amorphous or polycrystalline targets composed of a single element. While it met with some success in predicting sputtering yield in such systems, the transport theory breaks down in more complex systems.

At high rates of energy deposition, virtually all molecules are rapidly set into motion in a volume surrounding the path of the incoming particle. The collisions in the affected volume are too violent and too numerous to be described as individual binary events and Boltzmann transport theory can no longer be applied; instead, both

thermodynamic and mechanical models have emerged to describe sputtering under these conditions. Reimann has provided an excellent review.[20]

From the thermodynamic perspective, the rapid acquisition of significant kinetic energy by nearly every particle leads to the notion that the energized region is a "thermal spike" that can be characterized by a temperature T. A thermal spike's spatial expansion and temporal dissipation can be described by the formalism of heat conduction. Activated desorption and bulk desorption are two possible mechanisms that have been invoked to account for the ejection of material in response to a thermal spike. Under activated desorption, molecule-by-molecule evaporation is considered to take place from the heated region, while under bulk desorption, vaporization and emission of the entire spike region are considered to occur impulsively.

From the mechanical perspective, the rapid deposition of appreciable energy into a small volume leads to the notion that the resulting high energy density region is an "elastic spike" bounded by a steep energy density gradient. Both shock wave and pressure pulse formalisms have been used to describe this energy's propagation into the surrounding medium and its manifestation as kinetic energy of the sputtered particles. The shock wave models are based on the idea that supersonic propagation of the energy density gradient as a mechanical disturbance leaves the material in a heated or pressurized state from which desorption follows by evaporative or bulk desorption mechanisms or by impulsive release of compressive energy. The pressure pulse model

treats the propagation of the energy density as a simple diffusion process; in this formalism the energy density's steep gradient behaves as a time dependent volume force, or a pressure pulse, that imparts momentum to the molecules over which it passes. Although the calculational details are different, the shock wave formalism apparently reduces to the pressure pulse model in the limiting case of weak shocks.[21]

The bulk desorption, shock wave, and pressure pulse models are all good candidates for describing the physical aspects of the desorption phenomena reported in this thesis. Of these, the pressure pulse model may be the most appealing since it accounts more directly than the other two models for many of the sputtering effects observed in keV atom and ion bombardment of organic targets.[20]

1.1.5 Ionization Mechanisms in LSIMS

The sputtering process does not produce analytically useful ions.[8] Proposed mechanisms for the origin of the ions analyzed in LSIMS describe two distinct realms of ion formation: solution and the high energy gas-like region above the impacted surface referred to by Cooks as the "selvedge."[5] It is generally accepted that species existing as ions in solution may be desorbed directly into the gas phase by the sputtering process. Ions of this type usually provide the largest ion currents in analysis by liquid matrix assisted SIMS. Alternately, the prominent $(M+H)^+$ and $(M-H)^-$ ions commonly observed in liquid matrix assisted SIMS spectra, positive and negative ion

detection modes respectively, can be either the result of the transfer of labile protons from the solvent to dissolved molecules in solution or through collisions in the gas-like selvedge. Evidence has been reported supporting both mechanisms.[22,23] Watson et al. have qualitatively correlated ions detected in SIMS with protonation of a porphyrin molecule in solution as observed by visible spectroscopy.[24] On the other hand, Kebarle has demonstrated that for some classes of compounds gas phase basicities can be used to predict relative $(M+H)^+$ yields, thus supporting formation by ion-molecule reactions in the selvedge.[23] It is generally observed that increasing the acidity of the sample solution nearly always increases the ion current due to protonation, while deprotonation is favored in basic solutions. Cationization with species other than H^+ is seen to occur. Particularly common are ions formed by the attachment of Na^+ or K^+, species ubiquitous in biological samples. Addition of ammonium, silver, or alkali metal salts to the sample solution promotes cationization of this type. Again, however, solution as well as selvedge reactions may be operative here.

Although one electron processes are not common in liquid matrix assisted SIMS they have been reported for a number of analytes with low redox potential such as quinones.[25] Dienzer et al. have detected one electron reduction products by deconvolution of the molecular ion isotope patterns of oligonucleotide amide analogs.[26] The reducing equivalents for these processes are thought to be provided by the primary beam itself. Polycyclic aromatic hydrocarbons have been shown to yield high abundances of radical cations by liquid matrix assisted SIMS.[27] Radical ion formation

from primary radiation induced reactions have been reported, particularly at high primary radiation doses or prolonged bombardment.

1.2 Surface Phenomena

Particle induced desorption/ionization methods are fundamentally surface techniques. In both liquid and solid matrices, the particles are sputtered from a surface layer on the order of a few nanometers in thickness. The energy of the primary particle is effectively dissipated in this layer and has little effect on the bulk material beneath. Of course, once the surface layer has been sputtered away, a new surface is exposed for further sputtering. This can lead to temporal variations in the resulting spectra under intense or long term bombardment, particularly when the composition of the bulk material differs significantly from that of the surface layer. Alternately, temporal variations in spectra may be the result of debris generated from initial sputtering events that remain in the surface layer. In static SIMS an organic analyte is usually adsorbed onto the surface of a solid matrix. In this case, the relationship between surface and bulk compositions is well understood. In solutions, however, the relationship between surface and bulk compositions is a function of solvent-solute interactions that are not always well defined. In most solvent-solute systems the solute will to some extent behave differently in the two realms. A solute which preferentially resides at the surface of solution in a desorption matrix such as glycerol will present more molecules in the surface layer to be sputtered, and therefore analyzed, than another molecule

which has a greater affinity for the bulk of solution even though they are nominally present at the same bulk concentration. This rationale is used to qualitatively explain differences in sensitivity between and within various classes of compounds to particle induced desorption/ionization techniques. While the importance of surface phenomena has long been recognized with regard to these techniques, they have usually been regarded as complications in detection and quantitation. In order to fully understand these effects on, specifically, liquid matrix assisted SIMS a brief overview of solution surface chemical principles is desirable. Theoretical treatments of surface phenomena can be found in several excellent texts.[28,29] For this thesis, a few pertinent concepts will be defined and discussed without rigorous theoretical development as this is outside the scope of this study.

1.2.1 Surface Excess and Surface Activity

In the current context, "surface activity" is taken to be that property of a solute that produces a surface excess (or deficiency) of the solute in an arbitrarily defined surface layer relative to the bulk concentration in a given solvent.[30] In order to understand how the surface layer is defined, consider a property, P, as expressed in two phases, α and β, and follow its change as we move along a direction, x, normal to the interfacial boundary. If the boundary is truly a surface in the mathematical sense, then P would remain at a value, P_α, characteristic of the bulk α until it reached the surface, x_0, and change discontinuously to P_β upon crossing the infinitesimally wide boundary.

In reality, the surface has a finite thickness across which the change takes place continuously. This is illustrated schematically in figure 1.2a. The approximation of the surface as a plane with no thickness is reasonable if x_0 is placed such that the amount by which P is overestimated due to extending P_α to x_0 is the same as that by which it is underestimated due to extending P_β in a similar matter. In terms of the diagram, the shaded area to the left of x_0 should be equal to that on the right of x_0. Though arbitrary, such a placement of x_0 has the advantage of defining the surface such that there is no surface excess of property P. Placement of x_0 at any other point along x would result in a net excess or deficiency of P at the defined surface. Figure 1.2.b represents a phase, α, consisting of two components. Again, somewhat arbitrarily we can designate one component the solvent and the other the solute as is most convenient to the purpose at hand. Each component would have a value of property P. If, as illustrated, the change in P as a function of x for one component is not co-symmetric with that for the second component, the choice of location for x_0 becomes even more arbitrary. To study solute behavior it is convenient to place x_0 such that the surface excess of the solvent equals zero.

Using activity (or concentration) as the property P, the surface excess, Γ, of the solute when $\Gamma_{solvent} = 0$ is given by the Gibbs equation:

$$\Gamma = (-a/RT)(d\gamma/da)_T, \qquad (1\text{-}2)$$

Figure 1.2 Surface excess of a single component system (a) and a two component system (b).

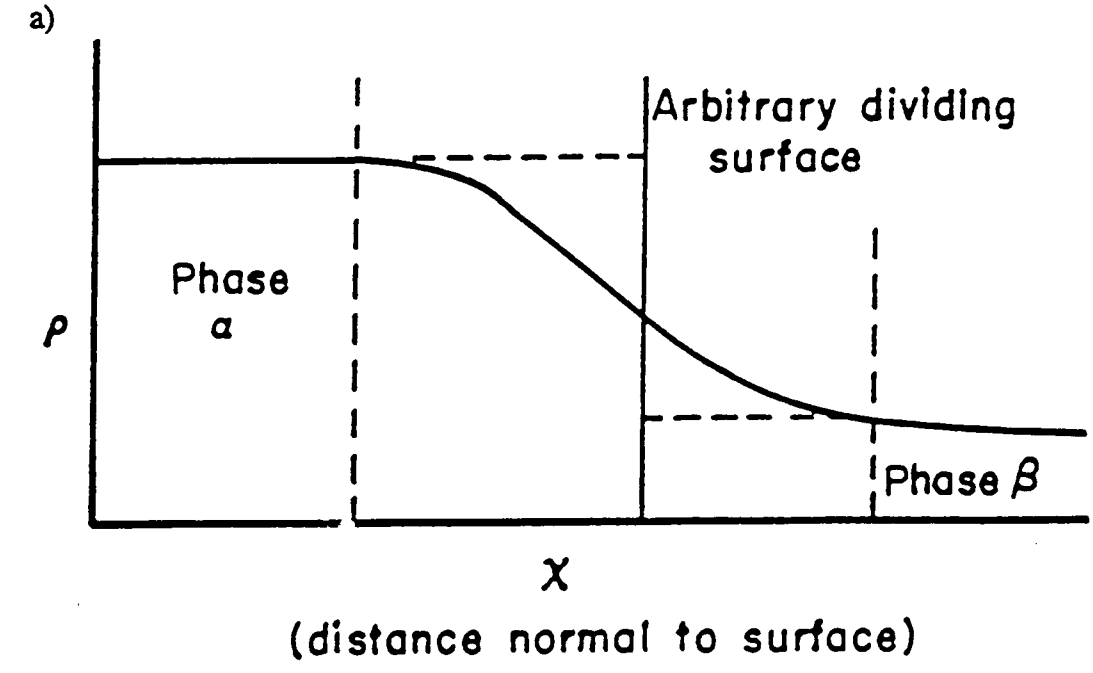

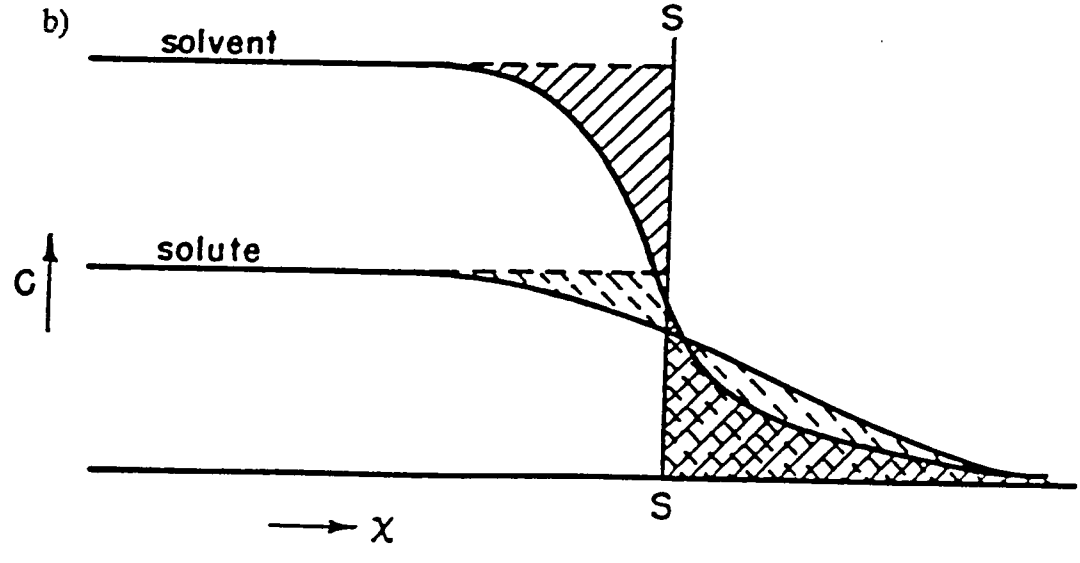

where γ is the surface tension and a is the activity of the solute in the bulk solution. For surface adsorption from dilute solutions the activity coefficients approach unity and concentrations may be substituted into the above equation.

1.2.2 Surface tension

Surface tension is conveniently thought of as a measure of the intermolecular attractions of the molecules at the surface of a liquid. Highly polar molecules, such as water and glycerol, have strong intermolecular forces, due to dipole-dipole and hydrogen bonding interactions, and consequently high surface tensions. Compounds such as hydrocarbons have much weaker intermolecular forces at work and correspondingly lower surface tensions. Thermodynamically, surface tension, γ, is the measure of the work required to increase the surface of the liquid by a given area. The units, therefore, are those of work or energy per area, J/m^2, or force per length, N/m. Lowering of the surface tension is energetically favorable. Therefore, in a solution, molecules with lower intermolecular forces will tend to populate the surface.

1.2.3 Surfactants

The term "surfactant" is used to describe those compounds that exhibit marked tendencies to adsorb at a surface. In water and other highly polar solvents, classical surfactants have two prominent features that account for their surface activity. They

can be described by the general formula RX where X is a polar "head" group and R is a hydrophobic group such as an aliphatic hydrocarbon chain. The polar head group may be nonionic, anionic, or cationic in nature. Typical nonionic head groups in RX are -OH, -COOH, -CN, $-CONH_2$ and -COOR'. Anionic head groups are $-SO_3^-$ and $-OSO_3^-$. Cationic groups include $-NR'_3{}^+$ and $-NC_5H_5^+$ (pyridinium). Note that some nonionic head groups may become ionic depending on the pH of the solution.

While the polar head group is easily solvated in polar solvents, the aliphatic tail is not. It is energetically favorable, then, to minimize contact between the hydrophobic portion of the molecule and the polar solvent. Two means of doing this are adsorption at the surface and micellization. In the first instance the molecules orient themselves at the surface such that the polar head groups are in contact with the solvent and the aliphatic portions tend to reside away from the bulk of solution as illustrated in figure 1.3a. The behavior of the surfactant molecules at the surface can be described in terms of two dimensional phases analogous to the familiar bulk phases of gas, liquid and solid to the extent that a two dimensional form of the ideal gas may be employed using the parameter of film pressure, π, which is defined as the decrease in surface tension over that of the pure solvent resulting from the presence of the surfactant layer or film,

$$\pi = \gamma_0 + \gamma. \qquad (1\text{-}3)$$

Figure 1.3. Surfactant behavior at a liquid surface and the stages of monolayer compression. a) a gaseous surface state, b) liquid expanded state, c) liquid condensed state and d) solid state.

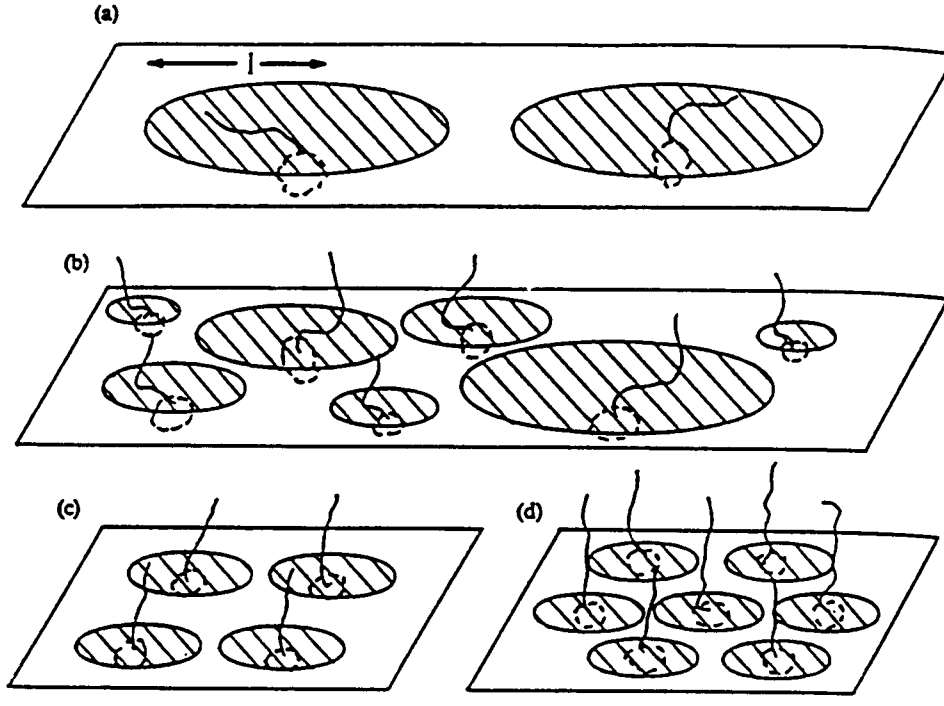

The lowering of the surface tension is a consequence of the aliphatic groups populating the surface having weaker molecular interactions than the solvent molecules they displace. Intuitively, it should be apparent that the surface concentration is a function of the bulk concentration to a maximum surface capacity defined by the minimum cross-sectional area taken up by the each individual surfactant molecule. This parameter is relatively independent of the aliphatic tail, but rather a characteristic of the polar head group. A typical adsorption isotherm is illustrated in figure 1.4 as constructed by Tajima et al. from β decay measurements at the surface of a solution of isotopically labelled sodium dodecylsulfate.[31]

Once the surface capacity has been reached further addition of surfactant to the solution concentration will eventually lead to micellization. The concentration at which micelles begin to form is called the critical micelle concentration or CMC. In micellization the hydrophobic tails of the surfactant molecules come together in a three dimensional structure with the polar head groups in contact with the solvent surrounding a hydrophobic domain. The interior of the micelle has properties similar to those of an oil droplet and can, itself, act as a nonpolar solvent for other hydrophobic species in solution. For ionic surfactants the micelle is typically composed of 10 - 100 individual molecules. Nonionic surfactants may form aggregates of thousands of molecules as they are not limited by the electrostatic repulsion of charged head groups.

Figure 1.4. Adsorption isotherm of sodium dodecylsulfate at air-solution interface.

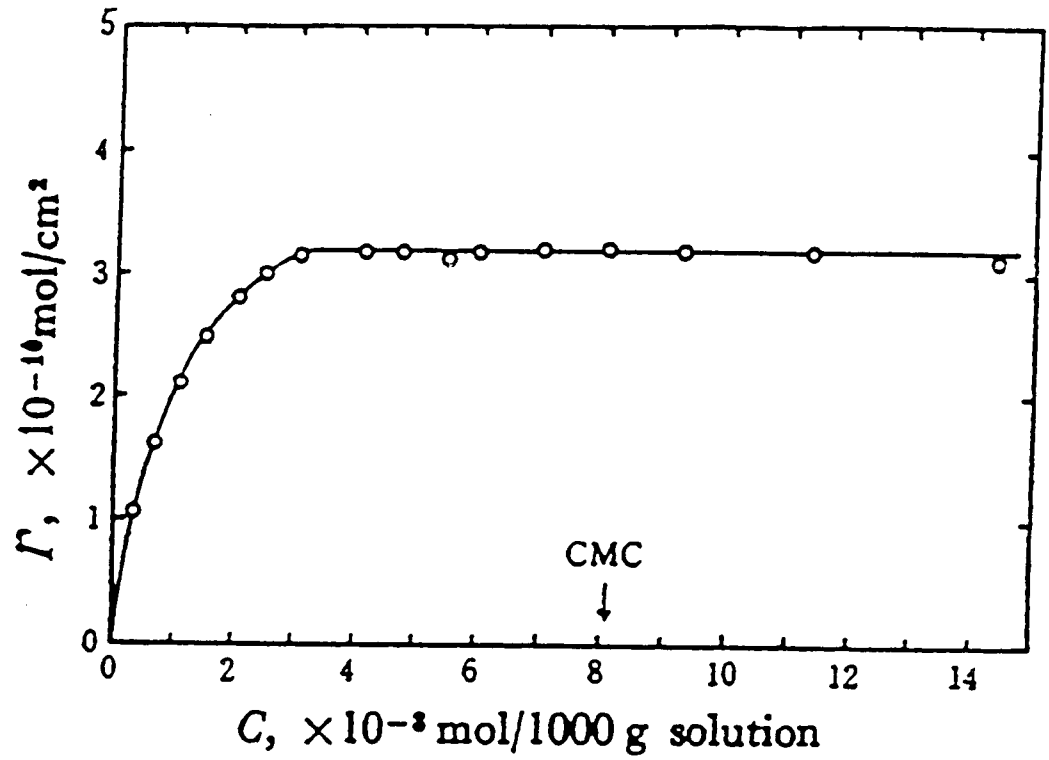

1.3 Consequences of surface phenomena on liquid matrix assisted SIMS

1.3.1 Surface activity and sensitivity

As previously stated, differences in sensitivity to liquid matrix assisted SIMS among otherwise similar compounds have long been attributed to differences in surface activity. A number of studies have sought to confirm this phenomenon usually with homologous series of increasingly aliphatic species. Ligon and Dorn have reported the detection of hexadecyltrimethylammonium bromide at a concentration of 10^{-6} M, five orders of magnitude less than that required to detect tetramethylammonium bromide despite the significantly greater mass of the former compound.[32] Similar effects have been reported for amino acids,[33] small peptides,[34] and fatty acids[35] in addition to numerous classical surfactants.[36] In all cases, when the chemistry is well behaved, surface activity accurately predicts the relative sensitivities in liquid matrix assisted SIMS.

A convenient measure of surface activity for species that can form micelles is the CMC. This concentration is intimately related to the solubility of the compound. In terms of mass spectrometry, the lower the CMC, the less bulk concentration is required to obtain monolayer coverage of the matrix, and therefore, the less sample is required to obtain the same sensitivity. For certain well behaved surfactants in aqueous

solution a quantitative relationship can be described between the CMC and the chain length of the aliphatic portion[37] as follows:

$$\text{Log CMC} = A - BN_C, \qquad (2\text{-}4)$$

where N_c is the number of carbons in the chain and A and B are empirical constants. CMC values have been reported for many compounds in aqueous solution. Less data is available for non aqueous systems although it is generally found that for organic solutes CMC values are somewhat higher in glycerol than in water.

1.3.2 Charge state and counterions

As well as chain length, any parameter that affects solubility will affect surface activity. Compounds with ionizable head groups will show a significant variation in surface activity with pH due to protonation or deprotonation of the head group. In the section on ionization it was stated that compounds that existed as ions in matrix solution generally provided the most intense ion signals in liquid matrix assisted SIMS. When the compound in question is surface active, however, decreasing the surface activity by forming a charged species could more than offset any advantage gained by the presence of preformed ions.[38]

Similarly, in the case of ionic surfactants, the nature of the counterion species may significantly affect the surface activity of the compound. Ligon has suggested that that ion which forms the least soluble salt should provide the greatest sensitivity in liquid matrix assisted SIMS.[30] The effect of counterions will be dealt with in depth in subsequent chapters as it is central to the current study.

1.3.3 Surface Renewal

It must be remembered that the surface of the sample solution is constantly being sputtered away during LSIMS analysis. The rate at which this takes place is a function of the primary particle flux density (or current density in the case of primary ions). Todd has determined that, for a primary ion current density of 1 $\mu A/cm^2$, removal of an octylamine film on glycerol occurs at a rate of 1 monolayer/7 seconds.[39] Without some mechanism for renewal of the surface excess at a rate comparable to that of depletion, the secondary ion signal will rapidly decrease to a value representative of the bulk concentration regardless of the surface activity of the solute. Surface renewal can occur through diffusion and convection. It is generally believed that diffusion through glycerol is too slow to effectively maintain surface excess of a surfactant under the primary ion current densities typically employed in LSIMS. Calculations have indicated that surface excesses would be rapidly depleted in a diffusion limited system.[40] In such a case, observation of effects due to surface activity would require conditions such as those used in static SIMS.

That surface effects are in fact observed in LSIMS indicate that renewal is not diffusion limited and can be explained by considering convective forces induced in the sample solution during particle bombardment. Convection can occur as a result of local heating during bombardment. The primary mechanism for convection in a sample solution containing surfactant, however, is the Marangoni effect. In this case, mixing of the surface and, ultimately, the bulk solution is driven by variations in film pressure, π, and surface tension, γ. Surface tension, it should be remembered, is a force acting in the plane of the surface to minimize surface area. Inhomogeneities in surface tension across the surface will lead to mechanical mixing of the surface layer as areas of high surface tension will be reduced at the expense of the surrounding areas of lower surface tension. Another way to view the situation is to consider film pressure exerted by the surfactant film which acts to reduce the surface tension. In a manner directly analogous to three dimensional pressure variations of gases, areas of high film pressure will expand over the surface at the expense of areas of low film pressure until the entire surface attains a homogenous film pressure. As film pressure is a function of surface concentration, local variations necessarily occur through individual sputtering events when a new surface having significantly lower surfactant concentration and, therefore, lower film pressure (higher surface tension, γ) is exposed. Convection of the bulk is induced due to the drag of the surface layer over the layers of bulk solution below it. The effect is magnified if the primary particle flux density is inhomogeneous over the sample surface area or if only a portion of the surface is irradiated. Ligon termed this effect "side filling."[30] The resulting convection significantly reduces the distance over

which diffusion must occur. Additionally, in solutions above the CMC of the surfactant, convective forces can effectively deliver micelles to the surface where they dissociate and spread rapidly across the surface.

1.3.4 Suppression effects

It must be noted that, while a surface active species is present at the surface in excess, compounds of lesser surface activity are necessarily displaced from that surface. This effect manifests itself in the resulting desorption-ionization process in what is known as the suppression effect. In a sample solution containing a single surfactant species in a glycerol matrix, the ion signals corresponding to glycerol ions, as well as the fragments and clusters thereof, are suppressed as the surfactant approaches monolayer coverage. Barber has shown that the concentration at which the glycerol signal is fully suppressed roughly corresponds to the point at which the surfactant reaches monolayer coverage as indicated by surface tension data.[35] In this instance, the suppression effect serves to decrease the chemical background due to the sputtering of matrix molecules and, therefore, enhances the signal to background ratio. In the analysis of mixtures, however, the suppression effect becomes problematic.

In a mixture of solutes, the compound with the greatest surface activity will tend to dominate the surface to the exclusion of the other solutes. The less surface active solutes will then have a surface deficiency. Though they may be present in sufficient

concentration to produce significant ion signal if alone in solution, these compounds may be undetectable in the mass spectrum of the mixture. This problem has been widely reported in the analysis of peptide digests.[41,42] Peptide fragments present in digests can vary widely in hydrophobicity and the more polar fragments may be completely suppressed in the resulting spectrum, thus complicating the accurate reconstruction of the original peptide. Although a more suitable technique was found for peptide digests using a solid matrix -- ^{252}Cf plasma desorption from a mylar backed nitrocellulose matrix -- the effect remains a problem for most mixtures in liquid matrix assisted SIMS.

Strategies for overcoming the suppression effect rely on attempts to minimize the differences in surface activity among the mixture components. These include selection of alternate matrices,[43] derivatization to increase surface activity of all components,[34] and for charged analytes, the addition of surfactants of neutral or opposite charge.[36]

1.3.5 Surface chemistry and sensitivity enhancement

It is not surprising in light of the previous discussion that strategies that rely on manipulation of surface activity to enhance sensitivity of liquid matrix assisted SIMS in the analysis of a compound are among the most successful. Obviously, optimization of surface activity should be considered when choosing a matrix. Surface activity may

be further enhanced by derivatization. Particularly, derivatization of polar molecules by the introduction of hydrophobic chains has been employed successfully both to enhance sensitivity of a single compound and to minimize differences in surface activity of compounds in a mixture. Derivatization schemes have been reported for many compounds including ketones,[44] amines[45] and peptides.[41,34]

Ligon and Dorn demonstrated the use of ionic surfactants as a means for enhancing the surface concentration of hydrophilic inorganic ions of opposite charge by ion pair formation.[46,47] In this technique, the charged surfactant is effectively transparent to the analysis when the detection mode is set for ions of opposite charge. For example, alkylpyridinium ions are not detected in negative ion mode. The counterion, however, is observed and at enhanced surface concentration. This technique was demonstrated to be effective in the analysis of several organic ions including adenosine triphosphate, ATP,[48] which is of particular interest in this work.

This laboratory is interested in the analysis of modified DNA constituents at pico- and femtomole levels. The report of a 1000 fold increase in sensitivity for ATP in the presence of n-hexadecylpyridinium acetate, HDPAc,[48] led us to study this phenomenon with a number of mononucleotides. To date, reports of sensitivity enhancement through ion pairing have been largely empirical in nature. This study attempts to describe the phenomena in terms of classical surface chemical theory.

Chapter 2

Methods

2.1 Instrumental

Two low energy (keV primary ions) modes and one high energy (MeV primary ions) mode of particle induced desorption-ionization were employed in this study. The two low energy modes are distinguished primarily by the flux of primary particles used to bombard a unit area of sample. In the so-called dynamic mode particle flux densities $\geq 6 \times 10^{13}$ particles/s•cm^2 and several monolayers of the target are sputtered per second; if secondary ion production is to remain stable for any appreciable period of time ($\geq$5 minutes) some mechanism, e.g. diffusion or convection is required for replenishing the removed surface molecules. In the so-called static ion mode, primary particle flux densities $\leq 10^{11}$ particles/s•cm^2 are used and 10 or more minutes are required to sputter a single monolayer of the target.

The instrument employed in this study for dynamic mode keV particle bombardment was a Kratos MS-50 double focusing mass spectrometer. Samples were introduced as ~ 2 μl of glycerol solution on a stainless steel sample probe having an area of ~ 10 mm^2. The target surface was bombarded by a beam of 8 keV Xe atoms produced by a Ion-Tech saddle field atom gun. Secondary ions were accelerated out

of the ion source to an energy of 8 keV. The mass analyzer consists of an electric and a magnetic sector in forward geometry. The magnetic sector field was scanned at a rate of 10 or 30 seconds per mass decade (an order of magnitude in mass range). Secondary ions are detected following post acceleration to 25 keV; both positive and negative ion detection is possible. Ion signals are centroided and masses are assigned using Kratos DS90 software.

The instrument employed in this study for static mode keV particle bombardment was a custom built time-of-flight mass spectrometer equipped with a liquid metal ion primary ion source.[49] Samples were introduced as tiny droplets of glycerol solution, typically of 0.3 to several nanoliters in volume, suspended on a 10 μm tungsten wire. The liquid metal ion source (FEI Corp.) supplies a 0.1 - 3.0 nA primary ion beam of 31 keV Au^+ ions. The primary ion beam was swept across the sample wire at a rate of 1000 to 2000 times per second. This procedure exposes the sample to only a few (10 - 100) primary ions per sweep cycle. The secondary ions released each sweep cycle are accelerated to 12 keV before entering a 30 cm field free flight tube. Ions are detected on a chevron microchannel plate assembly and counted using a LeCroy 4208 time-to-digital converter. Both positive and negative ions can be detected. The time to digital converter is cleared and started with each sweep of the primary ion beam; the converter is capable of counting up to eight detector events per start. Typically, data from 100,000 individual starts (i.e. passage of the primary beam over the sample) were summed to produce a spectrum. Data collection and analysis

were performed by an Atari Mega 4 computer using TOFMA software written by Dr. Werner Ens.[50]

High energy particle bombardment experiments were conducted by Douglas Barofsky and Judit Kopniczky at Uppsala University in Sweden on a ^{252}Cf plasma desorption mass spectrometer constructed at that University.[59] For this study, samples of 20 μl glycerol solution were smeared onto a Si target plate that was then placed on a probe and introduced through a vacuum lock into the ionization source. The primary particles, fission fragments of ^{252}Cf, impinge on the top surface of the target solution at an angle of 45°. Detection of the complementary fission fragment is used to start a time-to-digital converter. Secondary ions are accelerated to 14 keV and passed through a 90% transmission grid into a field free region heading toward the stop detector. Spectra were comprised of data collected from 400,000 starts. Data handling was performed on an Atari Mega 4 computer with the same TOFMA software used in the static keV experiments.

2.2 Chemicals

The nucleotides, adenosine triphosphate disodium salt ($ATPNa_2$), deoxyadenosine-5'-monophosphate (dAMP), deoxyguanosine-5'-monophosphate (dGMP), deoxycytidine-5'-monophosphate (dCMP), and thymidine-5'-monophosphate (TMP), were all obtained from Sigma chemical and used as purchased. The

monophosphates were obtained as the free acid. Perfluoroglutaric anhydride and n-hexadecylpyridinium chloride (HDPCl) were obtained from Aldrich Chemical Company. The highly branched C_{18} primary alcohol, 2,2,4,8,10,10-hexamethyl-5-hydroxymethyl-undecane was provided by W.V. Ligon of General Electric Company, Schenectady, New York. Glycerol was Aldrich reagent grade. Acetic acid, acetic-d_3 acid, and sodium acetate-d_3 were also purchased from Aldrich. Calf thymus DNA, deoxyribonuclease A, phosphodiesterase and alkaline phosphatase were purchased from Sigma. Anti-trans-7,8-dihydrodiol-9,10-epoxybenzo[a]pyrene, B[a]PDE, was purchased from NCI Chemical Carcinogen Repository at Midwest Research Institute, Kansas City, Missouri. Water was deionized using a Milli-Q deionization system (Millipore Corp.).

2.3 Preparation of n-hexadecylpyridinium acetate

20 ml dry volume of Amberlite IRA-410 strong basic anion exchanger, 40-50 mesh, Cl^- form, was prepared by washing the resin in H_2O and subsequently in methanol and packing it over glass wool in a 16 x 300 mm glass column. The resin was converted to its hydroxide form using 20 volumes of 1N NaOH. Following H_2O rinsing, the column was converted to the acetate form using 2 volumes of 1N acetic acid.

The column was then equilibrated to 50% methanol in deionized water with 5 volumes of the eluent. One gram (2.8 mmoles) hexadecylpyridinium chloride monohydrate was dissolved in 10 mL 50% methanol in deionized water. This solution was loaded on the column and eluted with 3 volumes (60 mL) of 50% methanol in deionized water. Methanol was removed by rotary evaporation. Water was removed by lyophilization to yield a waxy white powder of hexadecylpyridinium acetate, HDPAc. The procedure was repeated with acetic-d_3 acid to prepare the HDPAc-d_3. Glycerol solutions were made of the surfactant by dissolving the surfactant in water or methanol and mixing appropriate amounts with glycerol. The water or methanol was then removed under vacuum on a speedvac sample concentrator (Savant).

2.4 Preparation of anionic surfactant

The anionic surfactant, mono-[2-(2,2-dimethylpentyl)-5,12,12-trimethyl-1-octyl]-2,2,3,3,4,4,-hexafluoroglutaric (I) acid was prepared by combining 600 μl (4.5 mmoles) perfluoroglutaric anhydride and 1.2 g (4.5 mmoles) of the highly branched C_{18} primary alcohol without solvent and with stirring and cooling. The product was characterized by NMR and mass spectra and used without further purification. Glycerol solutions were prepared by dissolving the compound in dichloromethane and mixing with appropriate amounts of glycerol. The dichloromethane was subsequently removed under vacuum.

2.5 Synthesis of B[a]P-nucleotide adducts

One gram calf thymus DNA was suspended in 200 ml 0.05 M, pH 7.5 Tris (Sigma) buffer. It was then purified of RNA and protein contamination by treatment with RNAase and subsequent chloroform/isoamyl alcohol/phenol extraction, and precipitated with ethanol.[51] The purified DNA was resuspended in 400 ml 0.05 M pH 7.1 cacodylate buffer to a concentration of 0.75 mg/ml. Two 250 ml aliquots of this suspension were placed in 500 ml erlenmeyer flasks. To each flask was added 1 ml tetrahydrofuran (Burdick and Jackson) containing 2.6 mg B[a]PDE. The flasks were placed in a 37 degree water bath and shaken for two hours. Each suspension was then exhaustively extracted (12 x 125 ml) with diethyl ether (Burdick and Jackson) saturated with water. The DNA was precipitated with cold ethanol, pooled, and resuspended in 0.05 M, pH 7.5 Tris buffer. Extent of adduction of B[a]PDE to DNA was characterized by UV.

Enzymatic hydrolysis was carried out on 4 ml aliquots of the adducted DNA suspension. 200 μl 1.0 M $MgCl_2$ and 1250 units DNAase I were added to each aliquot and the mixtures were incubated in a 37 degree water bath for six hours. At that time 4 ml 0.1 M, pH 9.0 tris buffer was added with 0.4 units phosphodiesterase I and the mixtures were left to incubate at 37 degrees an additional 24 hours.

The mixtures were filtered and analyzed by HPLC on an ODS reverse phase, 4.6 x 250 mm column (Vydac 201TP104) with a 90 minute elution gradient from 100% water to 100% methanol at 0.65 ml/min. UV detection at 364 nm on a Spectroflow 783 UV detector (ABI/Kratos) was employed. The dGMP adduct eluted at ~32 minutes and was collected in a microcentrifuge tube. Solvent was removed by speedvac (Savant) and glycerol or HDPAc/glycerol was added before the sample went to dryness. Solvent removal continued until all water was removed. The resulting glycerol solution was ready for mass analysis.

2.6 Preparation of nucleotide samples

Nucleotide samples were prepared by preparing a stock solution of the nucleotide in water at a concentration of ~0.1 M. The stock solution was serially diluted and the dilutions mixed with appropriate amounts of glycerol to obtain concentrations of 10^{-6} to 10^{-2} M. Water was removed under vacuum using the speedvac sample concentrator. Samples prepared for analysis on the liquid metal ion source/time-of-flight mass spectrometer did not have water removed in this manner, but went into the mass spectrometer's vacuum lock with 10-20% water. It was assumed that the water was removed in the vacuum lock.

2.7 Software

Chemical equilibria calculations were carried out using MICROQL software, a basic program for calculating multicomponent equilibria written by John C. Westall.[56] In order to formulate the chemical equilibria problem for MICROQL, every chemical entity to be considered in the problem is defined as a species. A set of components is then defined such that every species can be written as a product of a reaction involving only components. As a chemical equilibrium problem is normally posed, the total (analytical) concentrations of all components are known as are the stoichiometry and stability constants of all species. This information is input to the software using the form illustrated in figure 2.1. The problem, which is to determine the free concentration of each species in solution, is solved by satisfying both the mass action and material balance equations.

The following is an example for a three component system. The components are M, R, and X. In solution the species will include M, R, and X as well as the component pairs MX and RX. Therefore, the two nontrivial equilibria are

$$M + X \rightleftarrows MX, \qquad (2\text{-}1)$$

and

Figure 2.1. MICROQL input matrix.

```
I. Components
    ##      Name      log X      Total []      TYPE
     1         M       -6.0          .001      Total Known
     2         R       -6.0          .001      Total Known
     3         X       -6.0          .001      Total Known

II. Species
##  Name      log K      M      R      X
 1  M          0.00      1      0      0
 2  R          0.00      0      1      0
 3  X          0.00      0      0      1
 4  MX         3.00      1      0      1
 5  RX         4.00      0      1      1
```

$$R + X \rightleftarrows RX. \qquad (2\text{-}1)$$

For each equilibrium a constant, K, can be defined. For example

$$K = [MX]/[M][X]. \qquad (2\text{-}3)$$

Solving for [MX] yields

$$[MX] = K[M][X], \qquad (2\text{-}4)$$

which can be expressed in logarithmic form as

$$\text{Log } [MX] = \text{Log } K + 1\text{Log } [M] + 1\text{Log } [X]. \qquad (2\text{-}5)$$

Note that in our example the stoichiometric coefficient for each component is 1 and is expressed explicitly in equation 2-5 for illustrative purposes. It should now be apparent that the input matrix in Section II of figure 2.1 is a list of mass action (equilibria) equations in the form of equation 2-5. For example, row #4 can be read

$$\text{Log } [MX] = \text{Log } K + 1\text{Log } [M] + 0 \log [R] + 1\log [X], \qquad (2\text{-}6)$$

where the value of each matrix element is the stoichiometric coefficient of that component in the equilibrium reaction. Thus, the matrix defines all mass action

equations to be considered. The material balance equations are read from the matrix vertically:

$$T_X = 1[X] + 1[MX] + 1[RX], \qquad (2\text{-}6)$$

that is the total X in solution must equal the sum of all species containing X. In section I of the input, total concentrations of the components are entered under "Total []", and "log X" is an initial guess for the free concentration of each component. The program then solves the problem iteratively from the initial guesses using a modified

Chapter 3

Results

3.1.1 Mass spectra of HDPAc

The positive LSIMS spectrum of n-hexadecylpyridinium acetate (HDPAc) is dominated by the HDP^+ ion at m/z 304 (figure 3.1a). At HDPAc concentrations above 1 mM in glycerol the matrix ions are virtually unobservable due to the suppression effect. Two series of minor peaks are seen at m/z = 304 + n(30) and 318 + n(30) where n is an integer. Keough attributed these series to reactions of the pyridinium species with radicals formed by beam induced fragmentation of glycerol.[52] In negative ion detection the surfactant ion is not observed (figure 3.1b). As in the positive spectra, suppression of the matrix peaks is seen at high HDPAc concentrations. The acetate anion is not detected.

3.1.2 Mass spectra of nucleotides

The mass spectra of various deoxynucleotides were recorded in both positive and negative ion detection modes on the Kratos MS-50 double focusing mass spectrometer. In positive ion mode deoxyadenosine-5'-monophosphate (dAMP) was virtually undetectable at a concentration of ~ 0.1 M in glycerol (figure 3.2). The addition of 0.2 N p-toluenesulfonic acid to the glycerol matrix provides an improved analyte signal due

Figure 3.1. LSIMS spectra of HDPAc in glycerol. a) positive and b) negative ion detection modes.

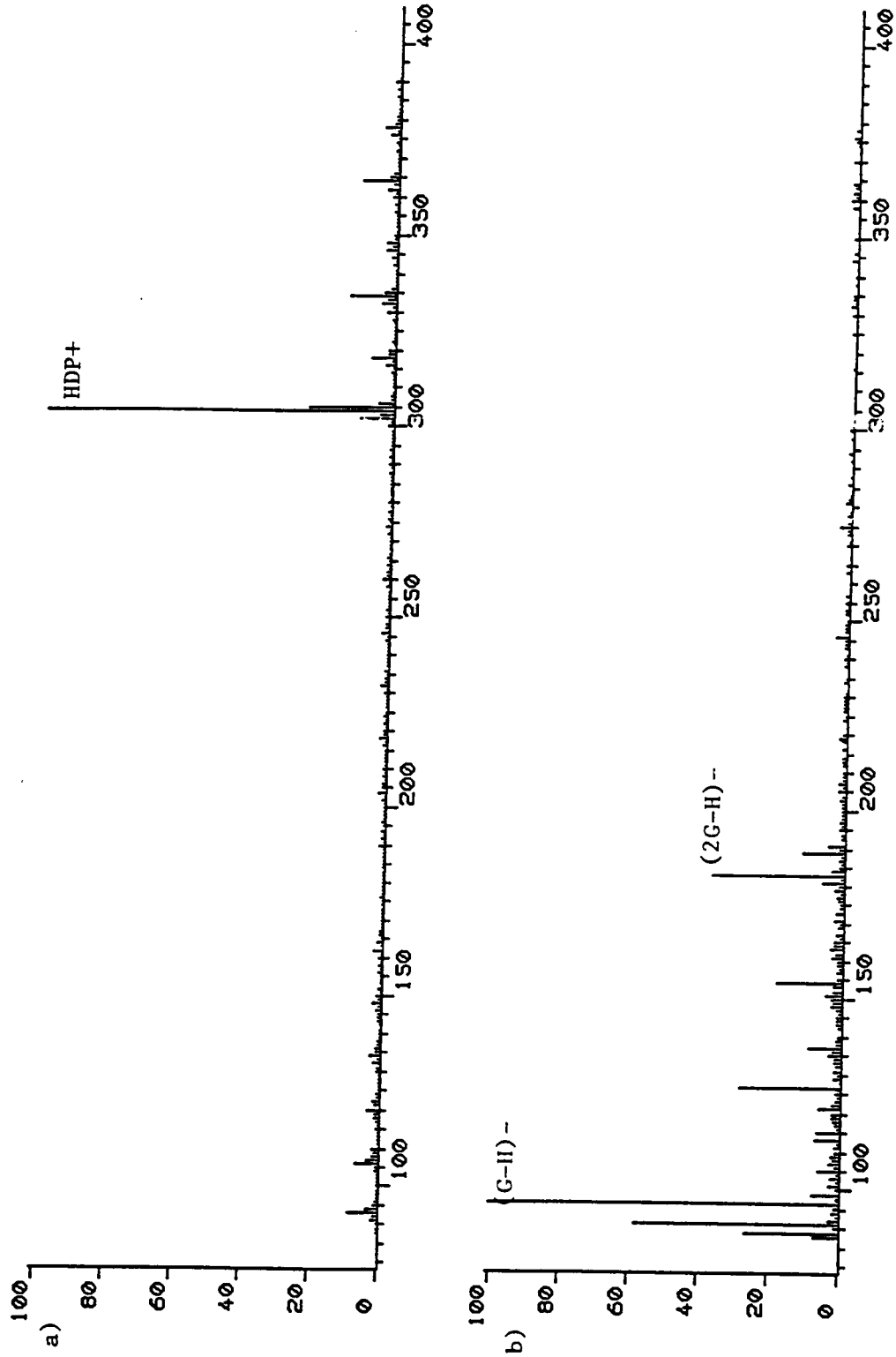

Figure 3.2. Positive ion LSIMS spectrum of dAMP in glycerol.

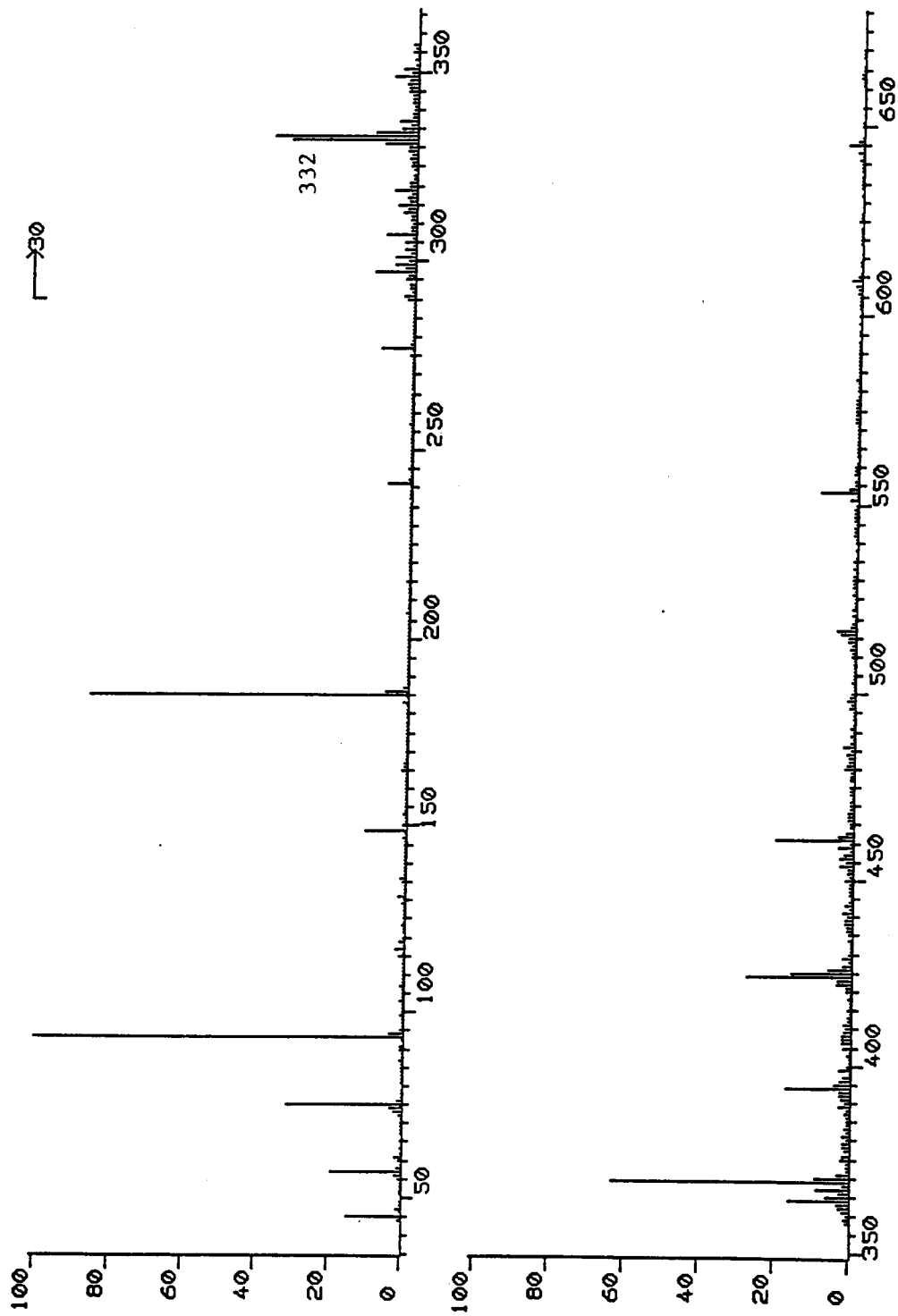

to the increased acidity of the sample solution (Moser and Wood). The characteristic mass spectra of deoxynucleoside monophosphates (figure 3.3) are dominated by the protonated molecular ion, $(M+H)^+$, in the positive ion mode. Cationization with sodium or another metal is also commonly observed in the presence of salts. In the current examples, however, none were detected. Also of significance in the positive ion spectra are the $(B+2H)^+$ where B represents the purine or pyrimidine base moiety of the nucleotide. This ion represents cleavage of the glycosidic bond with the transfer of a proton to the base moiety. In some cases this is the base peak in the spectrum. Additionally, $H_2PO_3^+$ can be observed at m/z 81. Other researchers have reported peaks at $(B+28)^+$ and $(B+30)^+$ resulting from cleavage across the deoxyribose ring structure.[53,54] These peaks, however, are not observed in sufficient abundance to be analytically useful.

Negative LSIMS spectra were obtained in glycerol (figure 3.4). An improved signal relative to that obtained in positive LSIMS in glycerol alone as matrix is to be expected since the phosphate moiety of the nucleotides is acidic and readily forms an anion in solution. The major peak is the $(M-H)^-$ molecular ion peak. The aglycone peak corresponding to the B^- ion is significantly reduced relative to the molecular ion and is, in fact, not readily observable in our spectra except in the case of thymidine monophosphate. Peaks corresponding to PO_3^- and $H_2PO_4^-$ can be observed at m/z 79 and 97, respectively.

Figure 3.3. Positive ion LSIMS mass spectra of a) dAMP, b)dGMP, c) dCMP and d) TMP in 0.2 N p-toluene sulfonic acid/glycerol.

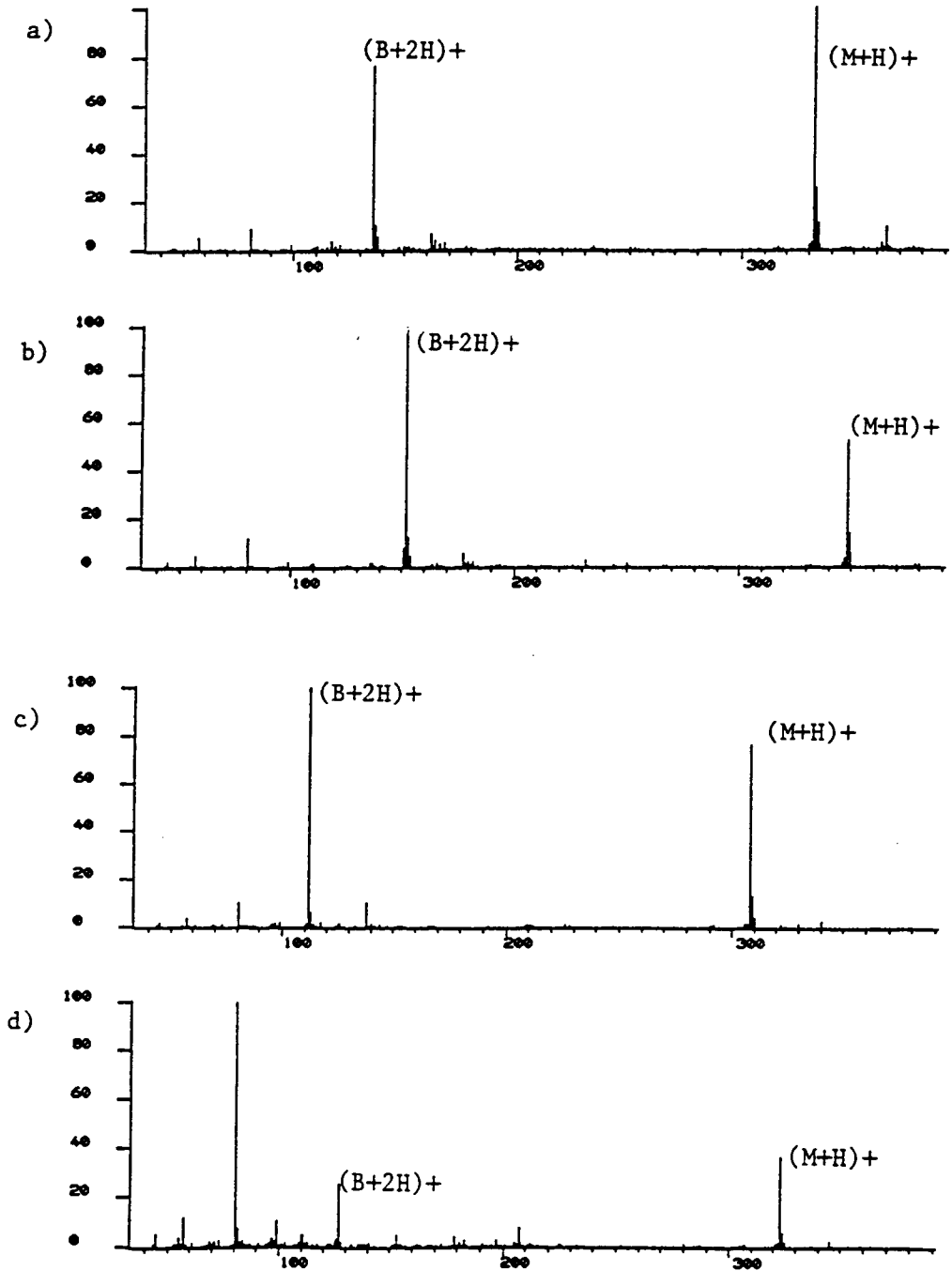

Figure 3.4. Negative ion LSIMS mass spectra of a) dAMP, b)dGMP, c) dCMP and d) TMP in glycerol.

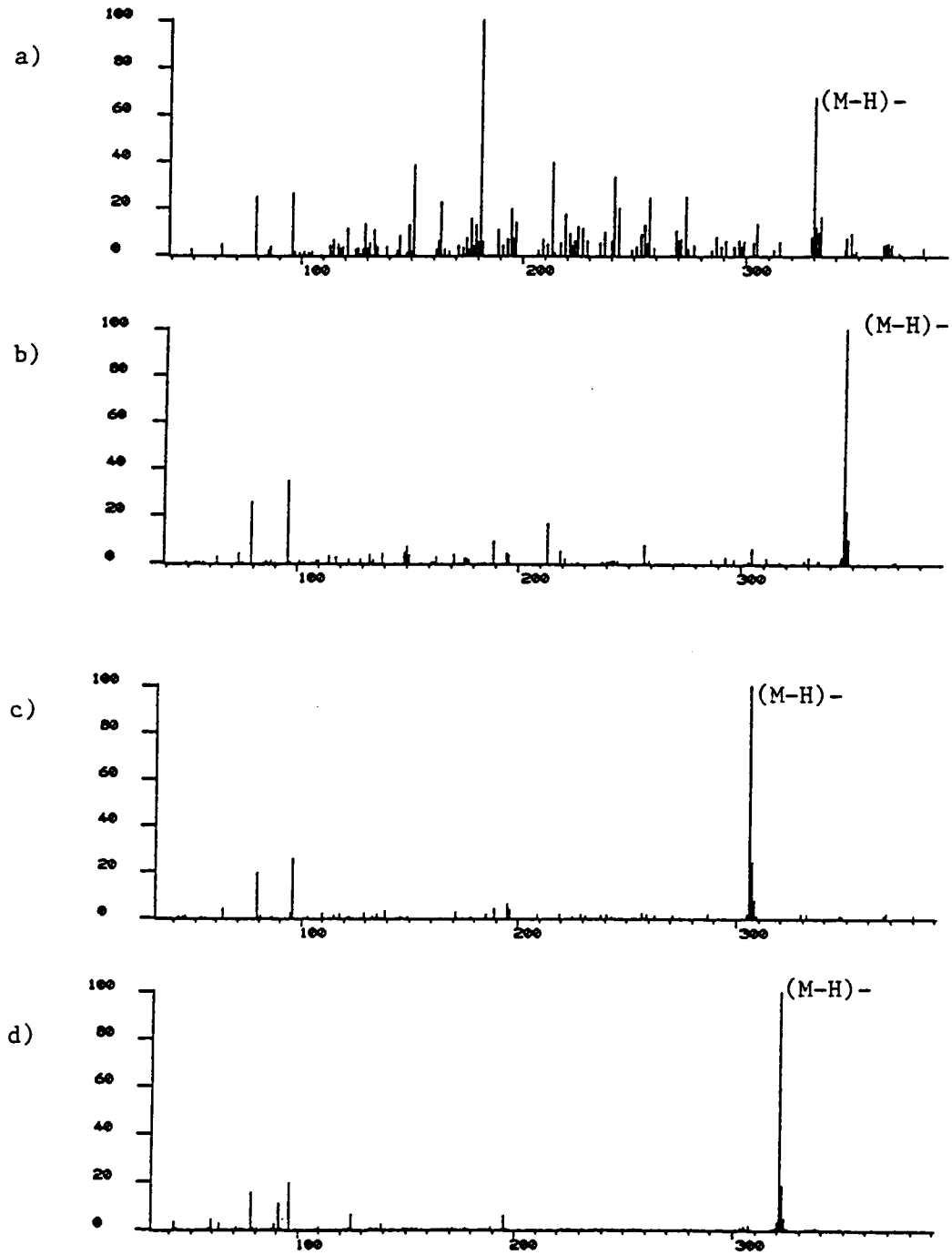

Adenosine triphosphate disodium salt (figure 3.5) yields $(M-H)^-$, $(M-2H+Na)^-$, and $(M-3H+2Na)^-$ due to the presence of multiple acidic hydrogens. No significant fragment ions are observed.

In the presence of 10 mM HDPAc/glycerol matrix, a 1 mM solution of ATP disodium salt gives a base peak of m/z 506 corresponding to the deprotonated molecular ion (figure 3.6). The sodiated molecular ions present in the spectrum taken from $ATPNa_2$ in glycerol alone are virtually undetectable. Significant fragment peaks are observed at m/z 426 and 408 corresponding to the loss of phosphate and the subsequent loss of H_2O from the resulting species, respectively. Two series of phosphate related peaks are observed at m/z 79, 159, 239 and m/z 97, 177, 257. The peak at m/z 59 is believed to be acetate, although a portion of the intensity may be contributed by a comassive glycerol fragment ion. The surfactant is virtually "transparent" to the analysis. Similar results were obtained for the monophosphates of deoxyadenosine and deoxyguanosine (figure 3.7). In addition to the ions previously observed, present in the spectra are peaks corresponding to $(M-B-2H)^-$ and $(M-2H+HDP)^-$.

3.2 Sensitivity and detection limit enhancement

Ligon and Dorn reported a 1000 fold increase in sensitivity for ATP in LSIMS in the presence of 1mM HDPAc in glycerol matrix.[48] This estimate of sensitivity enhancement was based on the sample concentration required to obtain "quality"

Figure 3.5. Negative ion LSIMS mass spectrum of ATP disodium salt in glycerol.

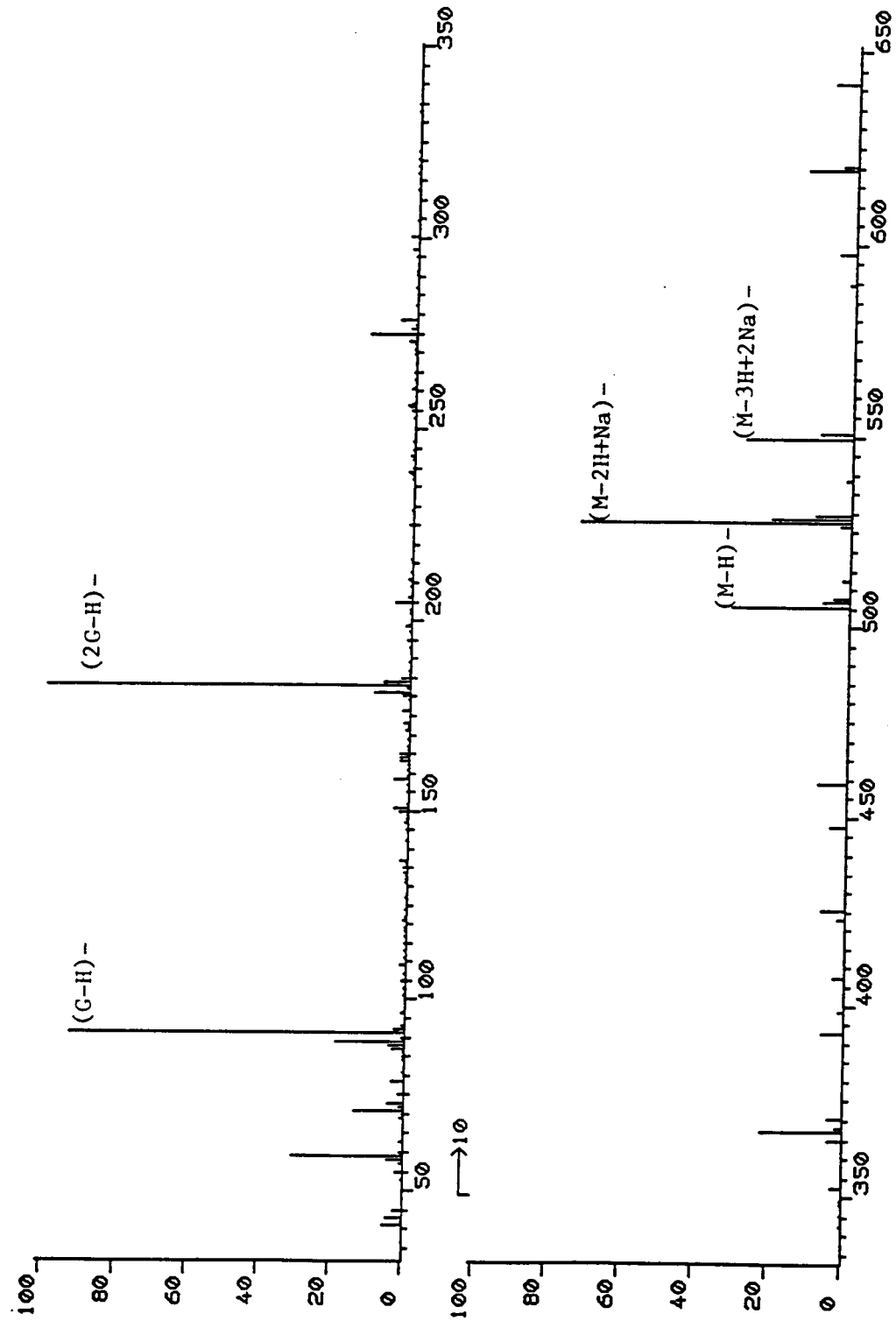

Figure 3.6. Negative ion LSIMS mass spectrum of 1 mM $ATPNa_2$ in 10 mM HDPAc/glycerol.

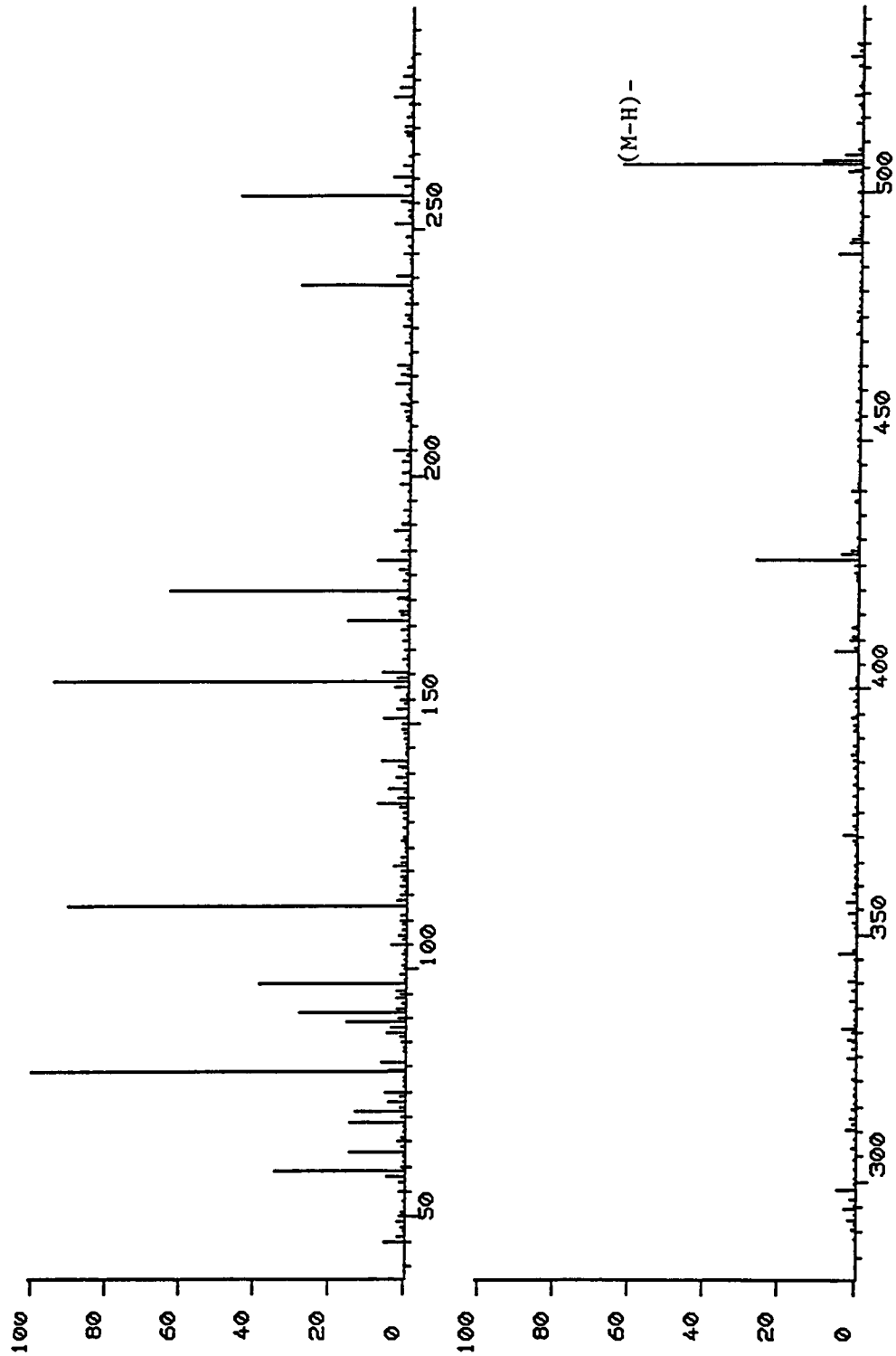

Figure 3.7. Negative ion LSIMS mass spectra of a) 1 mM dAMP and b) 1 mM dGMP in 10 mM HDPAc/glycerol.

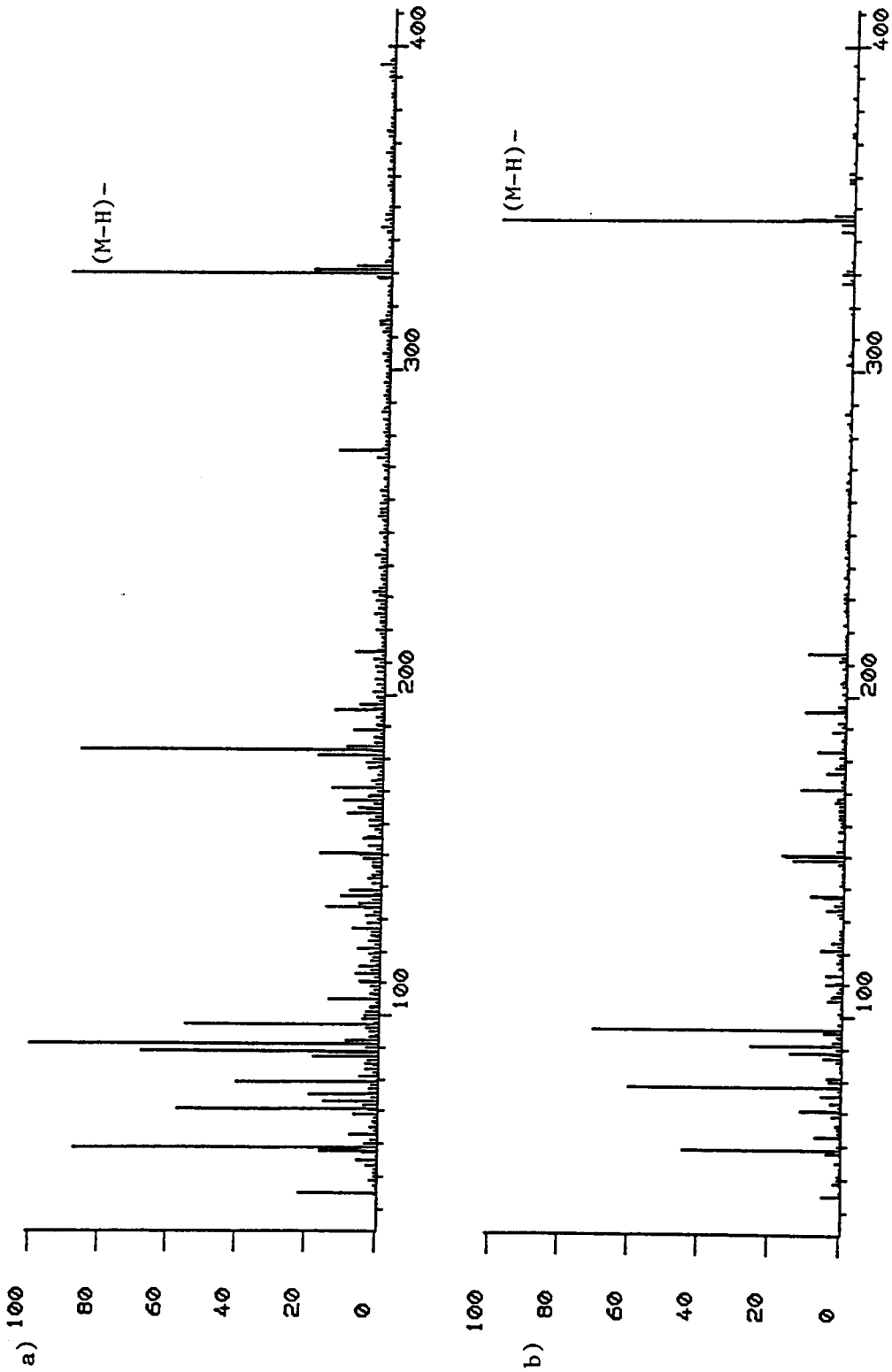

spectra, the molecular ion signal intensity, and the detector gain setting. They estimated that ATP in glycerol at a concentration of 10^{-2} M produced essentially equivalent spectra to those obtained from 10^{-5} M ATP in 1 mM HDPAc/glycerol. Our own attempts to verify these results yielded a more complex relationship. ATP/glycerol solutions were prepared at 10^{-2}, 10^{-3}, and 10^{-4} M concentrations, while solutions of ATP in 1 mM HDPAc/glycerol were prepared at concentrations of 10^{-2}, 10^{-3}, 10^{-4}, 10^{-5} and 10^{-6} M. Samples were analyzed under identical instrumental conditions. Sensitivity enhancement is calculated as

$$\text{Enhancement Factor} = \{[S/B]_s/[N^-]_s\}/\{[S/B]_0/[N^-]_0\}, \qquad (3\text{-}1)$$

where $[S/B]_0$ and $[S/B]_s$ are the signal to background ratio for the ion peak of interest, in this case m/z 506, in glycerol alone and in surfactant/glycerol, respectively, and $[N^-]$ is the concentration of the nucleotide. When centroided data is used ion intensities are used in place of [S/B]. Sensitivity is taken to be the signal to background ratio divided by the analyte concentration. Illustrated in figure 3.8 are the molecular ion regions of spectra taken of 10^{-2} M ATP in glycerol alone and in surfactant/glycerol matrix. Using equation 4-1, the sensitivity enhancement factor is 11. However, 10^{-5} M ATP in surfactant/glycerol gives an enhancement factor of 10^4 when compared to 10^{-2} M ATP in glycerol alone (figure 3.9). It is interesting to note that the ion signal produced by 10^{-5} M ATP in surfactant/glycerol is nearly the same as that produced by 10^{-2} M ATP

Figure 3.8. Molecular ion region of LSIMS mass spectra of 10 mM $ATPNa_2$ in a) glycerol and b) 1 mM HDPAc/glycerol.

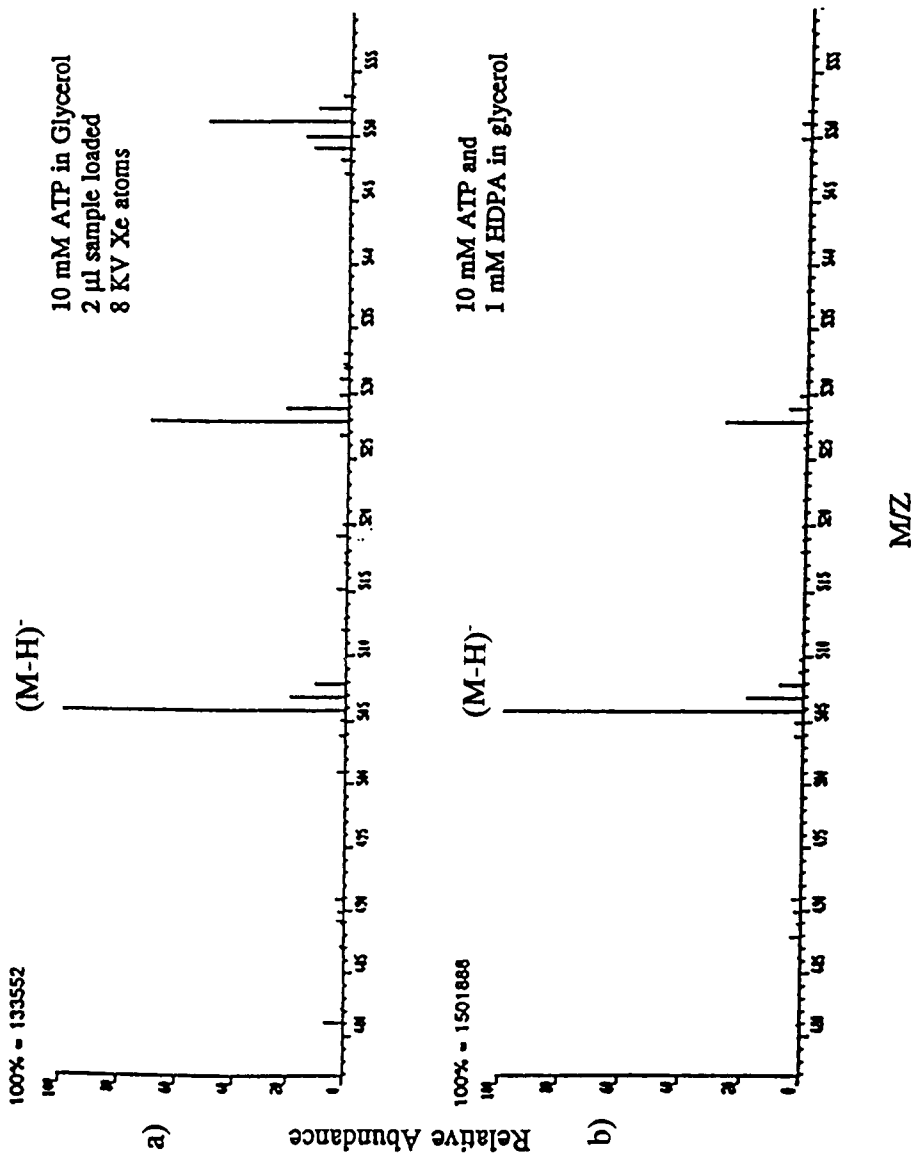

Figure 3.9. Molecular ion region of LSIMS mass spectra of $ATPNa_2$ at a) 10 mM in glycerol and b) 10 pM in 1 mM HDPAc/glycerol.

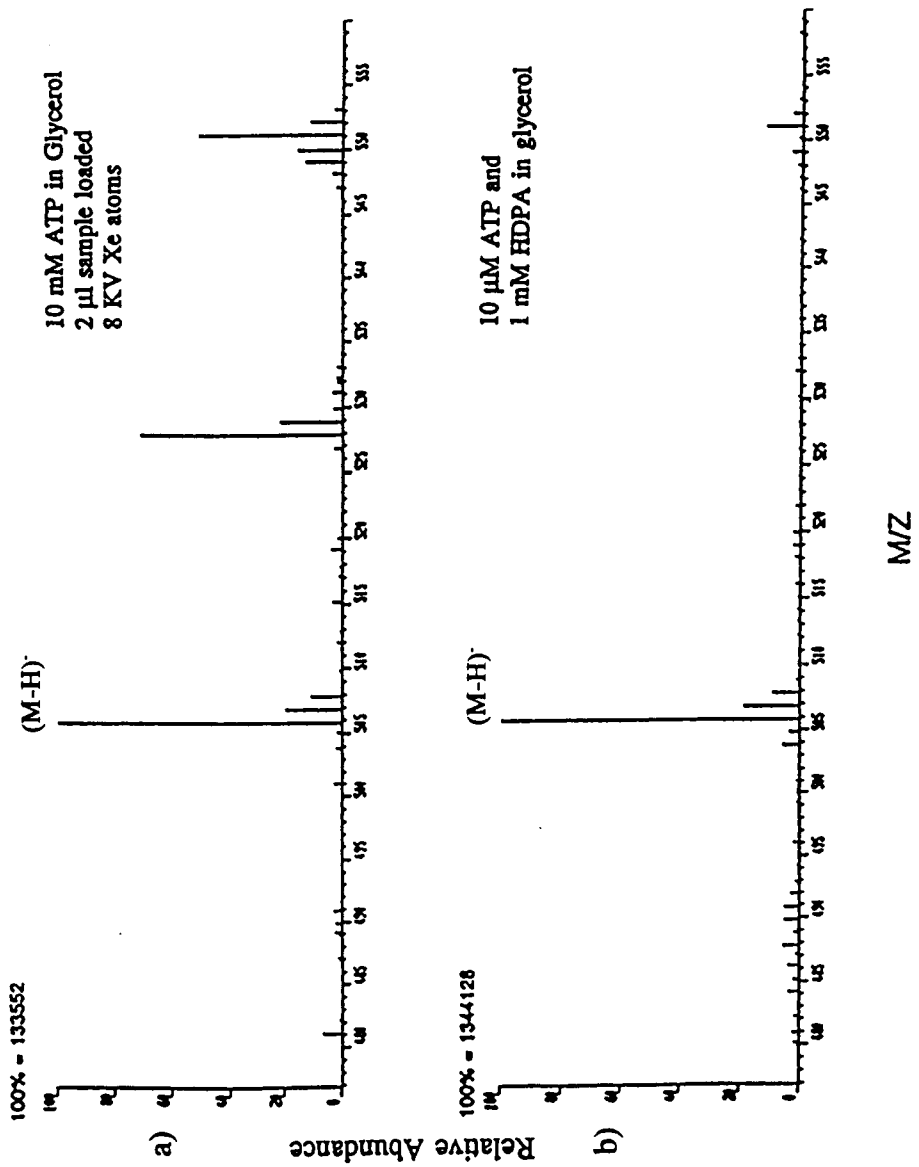

in surfactant/glycerol. Figure 3.10 shows the signal intensity as a function of analyte concentration for both series of samples. Clearly, in the presence of surfactant the analyte concentration is not the primary control of signal intensity. As previously stated, LSIMS samples the surface of the target solution. Therefore, the ion signal should be related to the surface concentration of the analyte. The surface composition of a surfactant solution is primarily governed by the amount of surfactant present in solution. Figure 3.11 illustrates this dependence for various analyte concentrations. The primary features of interest in this dependence are the nearly linear initial relationship, the optimum surfactant concentration which changes with analyte concentration and the decrease in signal intensity at surfactant concentrations above the optimum. The implications of this curve will be examined more fully in the next chapter.

The detection limit is operationally defined as the analyte concentration at which [S/B] = 2. The background is estimated, as per Watson,[55] by averaging the surrounding peak intensities excluding those attributable to analyte or matrix. A solution of 10^{-3} M ATP in glycerol alone produced a [S/B] of ~3 for the peak at m/z 506. In the presence of 10^{-3} M HDPAc in glycerol 10^{-5} M ATP gave a S/B for m/z 506 of ~5 (figure 3.12). It must be noted that 10^{-5} M ATP could not be detected at HDPAc concentrations of 10^{-4} or 10^{-2} M. the molecular ion region of these three spectra are shown in figure 3.13.

Figure 3.10. ATP (m/z 506) signal versus $ATPNa_2$ concentration.

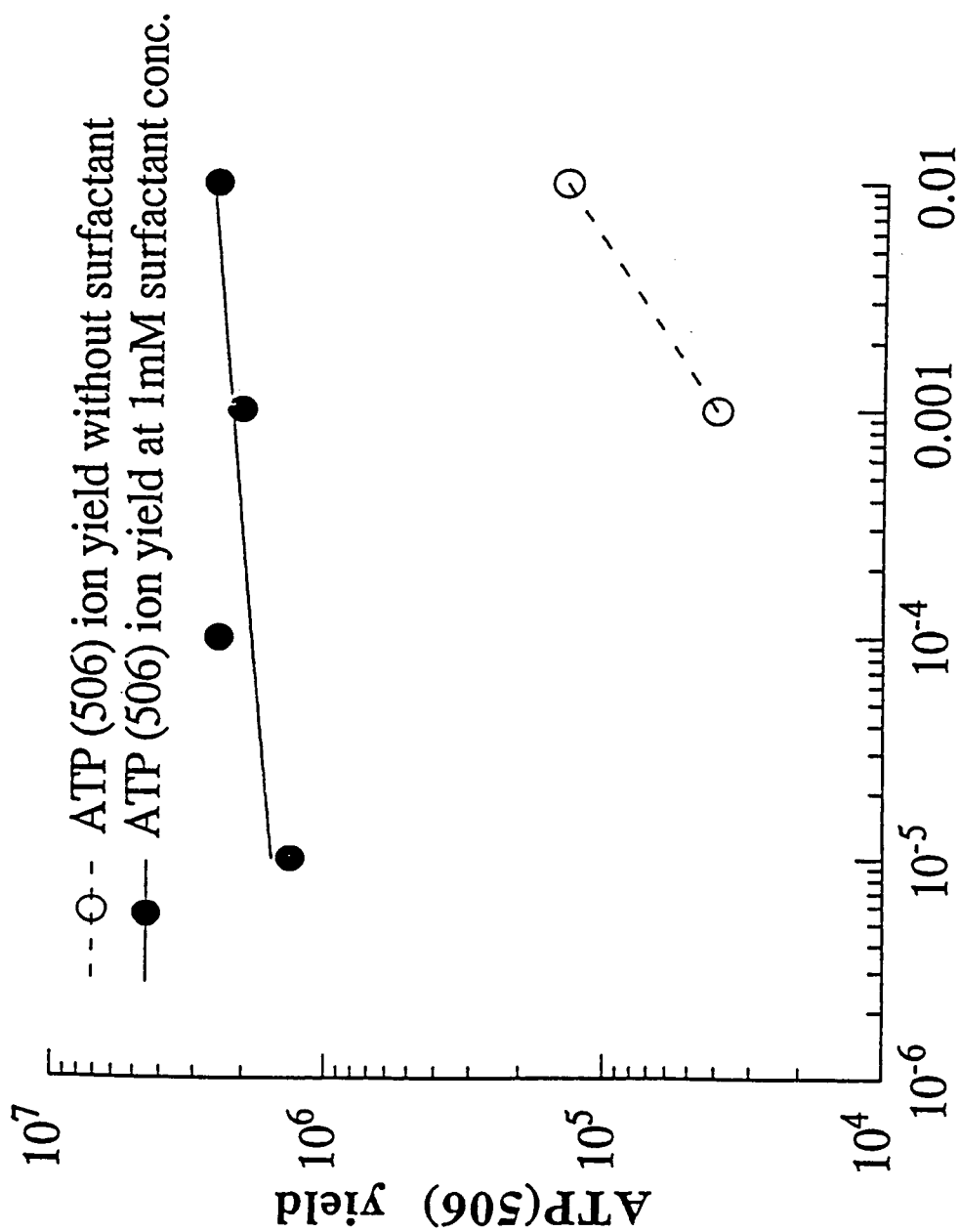

Figure 3.11. ATP (m/z 506) signal versus surfactant concentration.

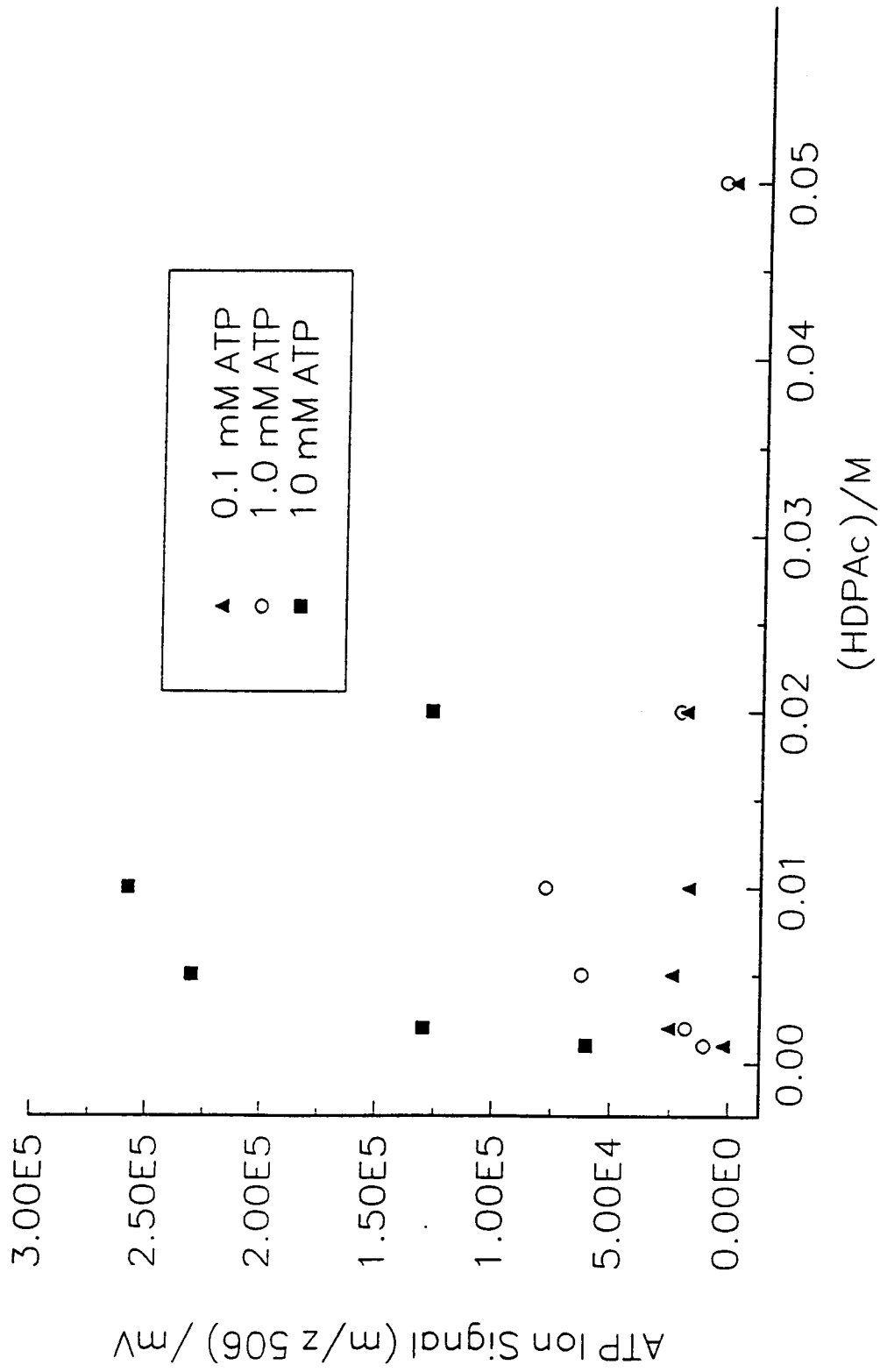

Figure 3.12. LSIMS mass spectra of a) 10^{-5} M ATP in 10 mM HDPAc/glycerol and b) 10^{-3} M ATP in glycerol.

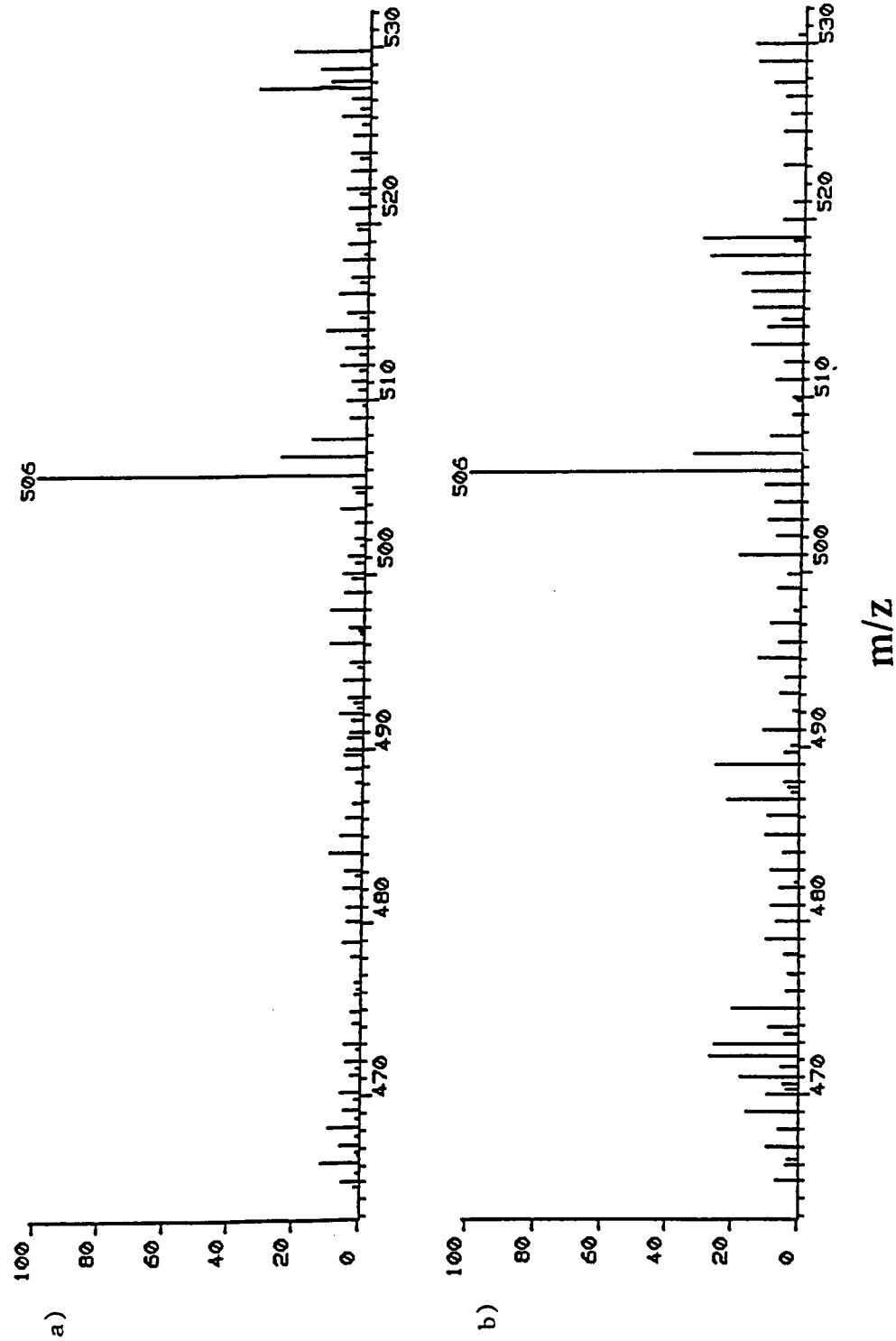

Figure 3.13. LSIMS mass spectra of 10^{-5} M ATP in a) 10^{-2} M b) 10^{-3} M and c) 10^{-4} M HDPAc/glycerol.

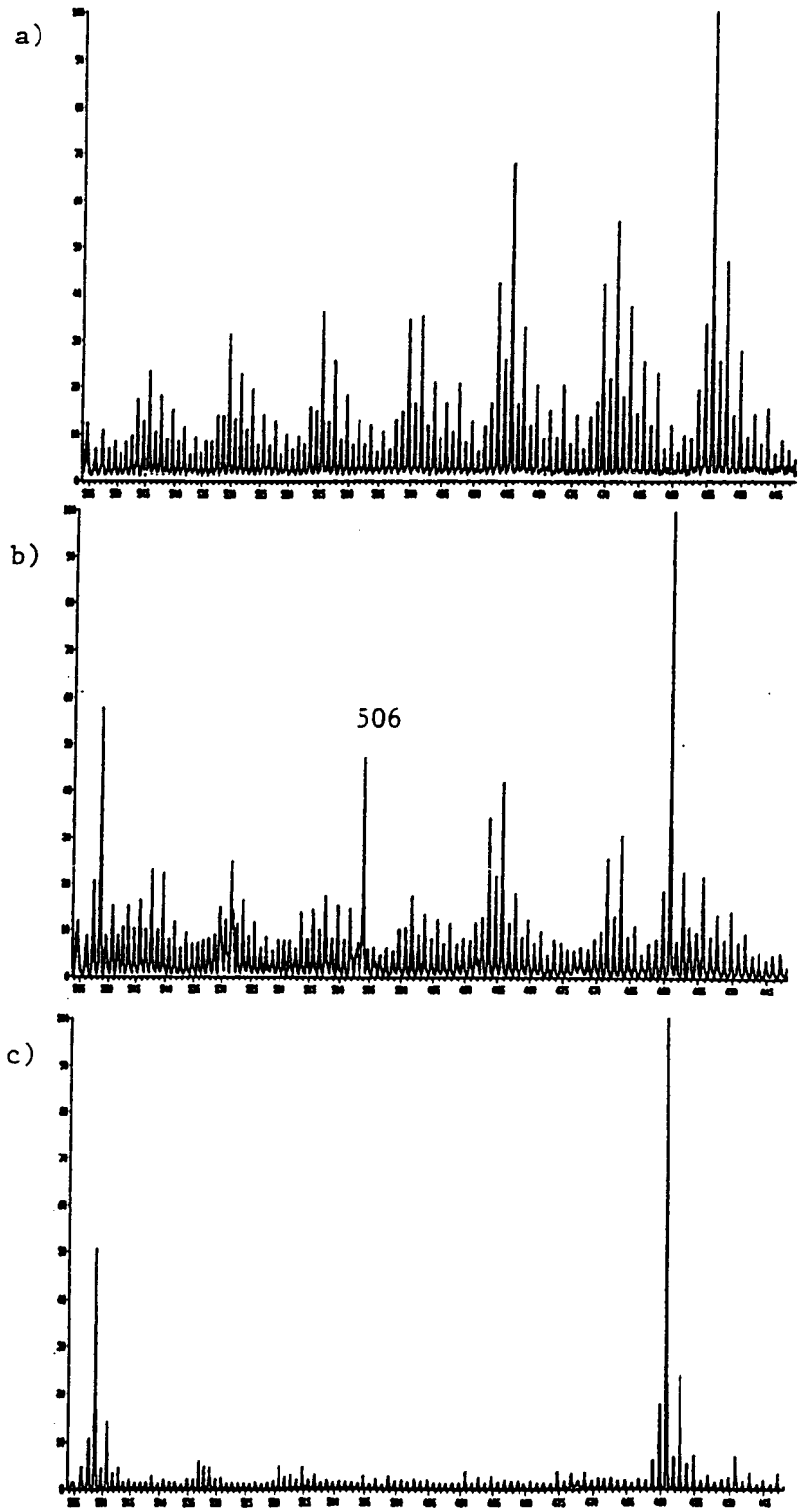

Deoxyadenosine-5'-monophosphate (dAMP) yielded similar results. Figure 3.14 shows the molecular ion region of the spectra of 10^{-3} M dAMP in glycerol and in 10^{-2} M HDPAc/glycerol. The enhancement factor in terms of the signal strength of the m/z 330 peak is 220. The signal produced from dAMP in glycerol alone is not above the background of the surrounding peaks. With careful background subtraction, however, we can estimate that the dAMP signal contributes approximately 75% of the ion intensity at this m/z. Therefore, the stated enhancement factor is conservative. The monophosphates exhibited the same surfactant concentration dependence as the triphosphate (figure 3.15).

3.3 Time-of-flight data

3.3.1 ^{232}Cf plasma desorption

In collaboration with researchers in Bo Sundqvist's laboratory at Uppsala University, Uppsala, Sweden, ATP solutions in 1 mM HDPAc/glycerol matrix were subjected to ionization by bombardment with fission fragments of ^{232}Cf in a time-of-flight mass spectrometer. The spectra obtained were essentially the same as those obtained by LSIMS. An additional series of minor peaks were observed in the spectra, however. These were determined to correlate to clusters of ATP with multiple HDP^+ associated. The ions detected were $(ATP - 2H + HDP)^-$, $(ATP - 3H + 2HDP)^-$,

Figure 3.14. LSIMS mass spectra of 10^{-3} M dAMP in a) glycerol and b)10^{-2} M HDPAc/glycerol.

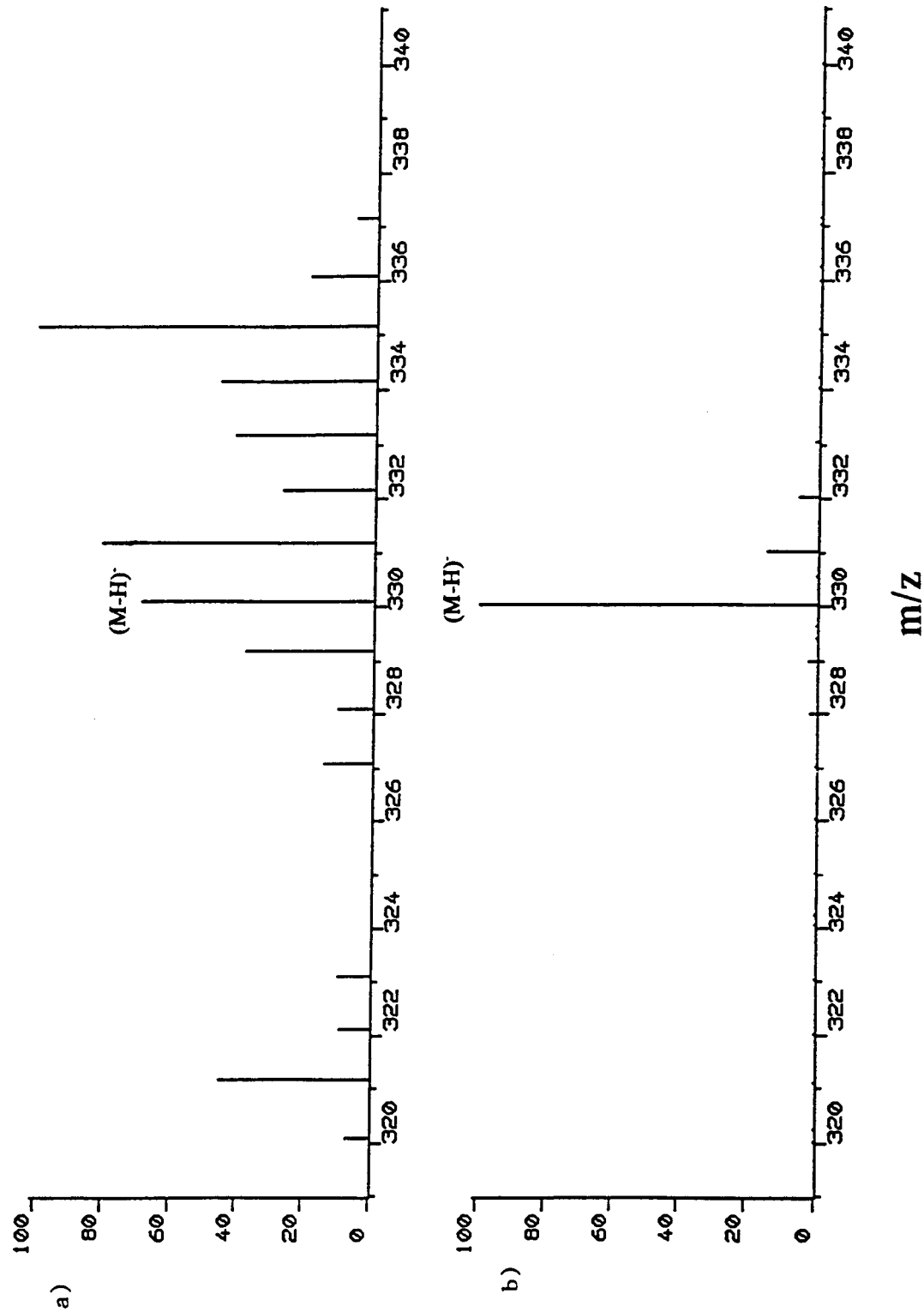

Figure 3.15. dGMP ion signal vs. surfactant concentration.

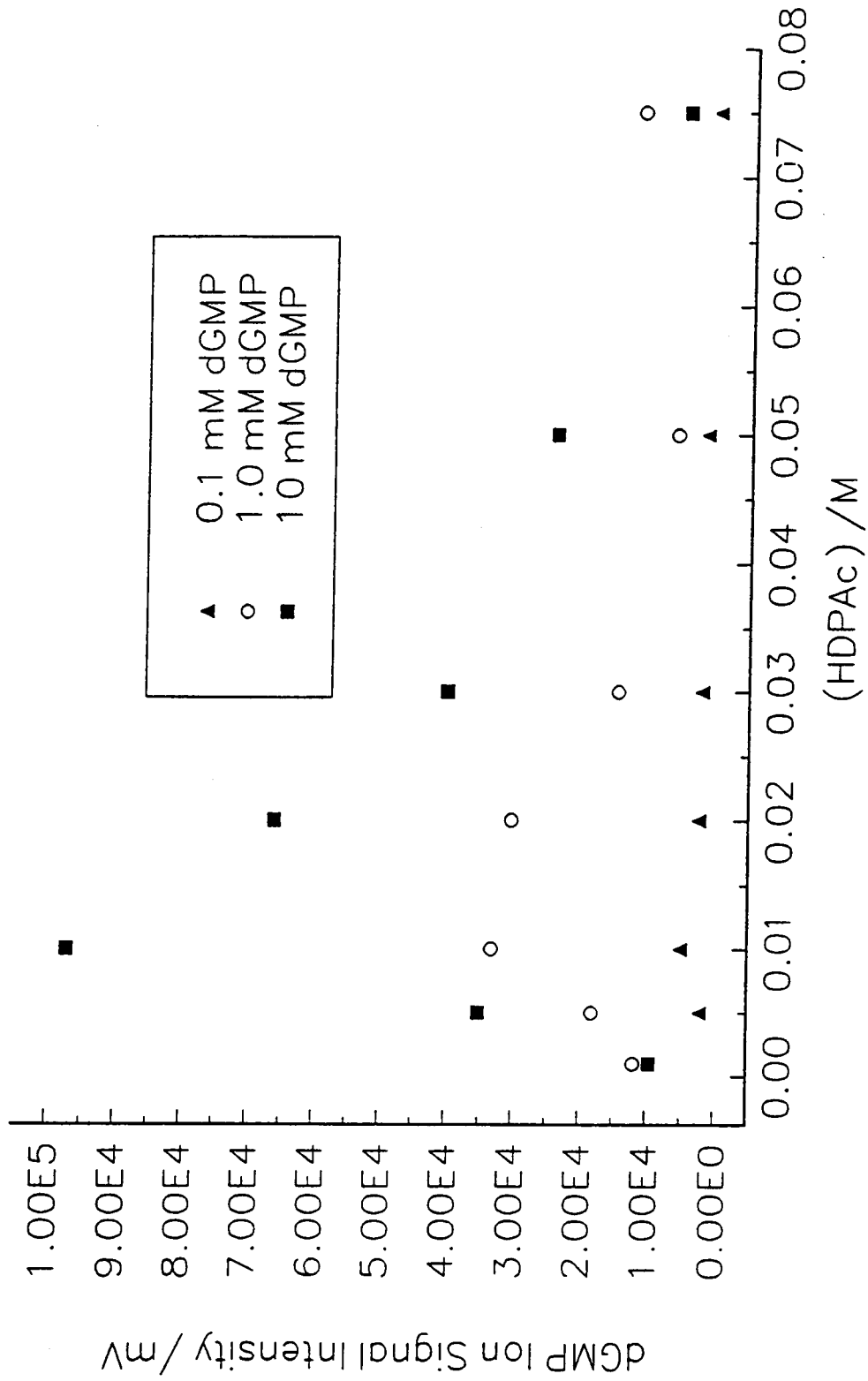

$(2ATP - 3H + 2HDP)^-$.... Each additional ATP can associate with up to three HDP^+ ions.

In terms of sensitivity enhancement a factor of 675 was calculated for ATP in glycerol with a surfactant concentration of 10^{-3} M. Similar concentration dependencies were observed (figures 3.16 and 3.17).

3.3.2 Liquid metal ion source LSIMS

The advantage of the surfactant/glycerol system was combined with the instrumental advantage of the liquid metal ion source LSIMS/time-of-flight mass spectrometer. The results were analogous to those obtained on the Kratos MS-50. The same surfactant signal dependence was observed (figure 3.18) as was expected since the two ionization techniques are fundamentally the same. The geometry of the ion source permitted loading of as little as 0.3 nanoliters of 10^{-5} M solutions dAMP and dGMP whereas 1 to several microliters is typical in a conventional LSIMS source. The resulting detection limit based on actual amount of sample loaded was in the low femtomole range (figures 3.19 and 3.20).

Figure 3.16. ^{252}Cf PDMS ATP ion signal vs. $ATPNa_2$ concentration.

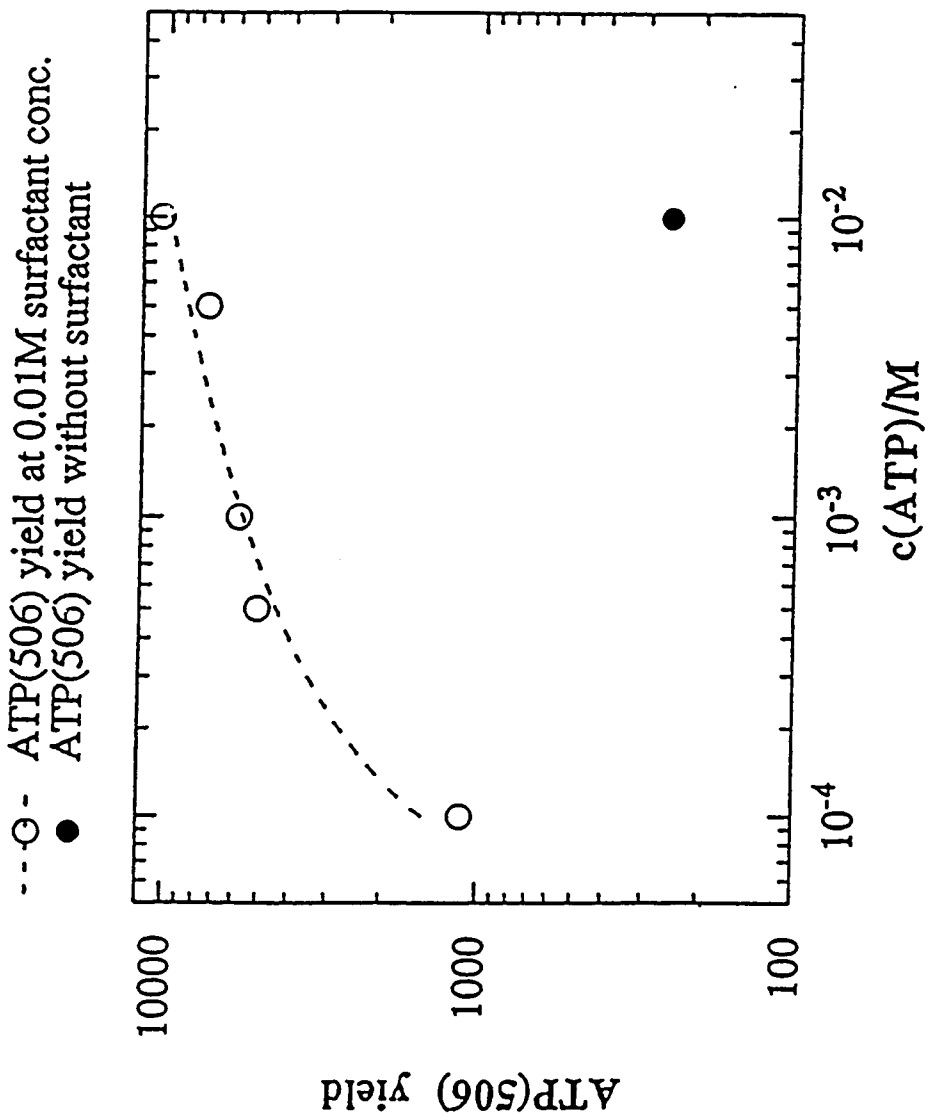

Figure 3.17. ^{252}Cf PDMS ATP ion signal vs. surfactant concentration.

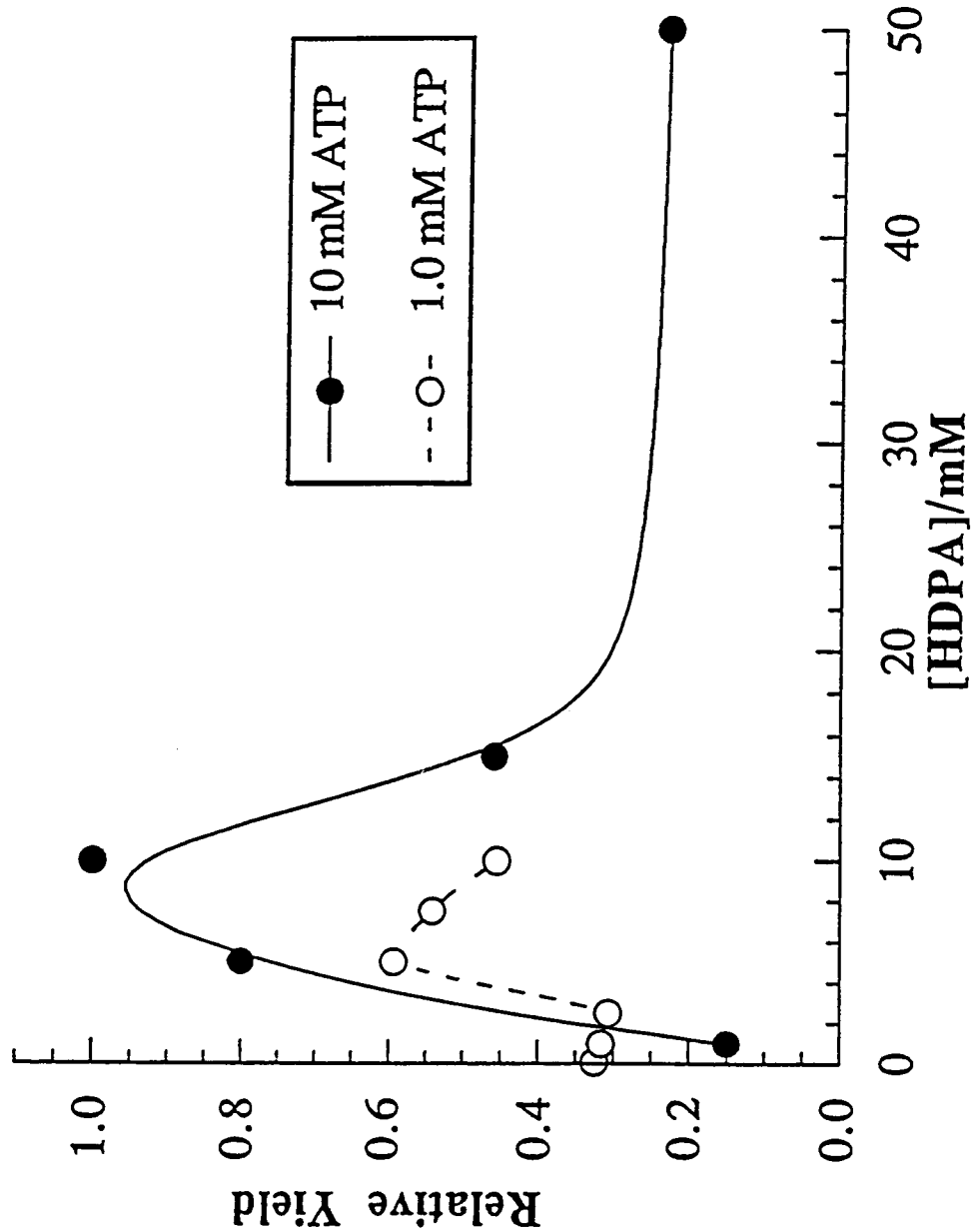

Figure 3.18. LSIMS/TOF dGMP ion signal vs. surfactant concentration.

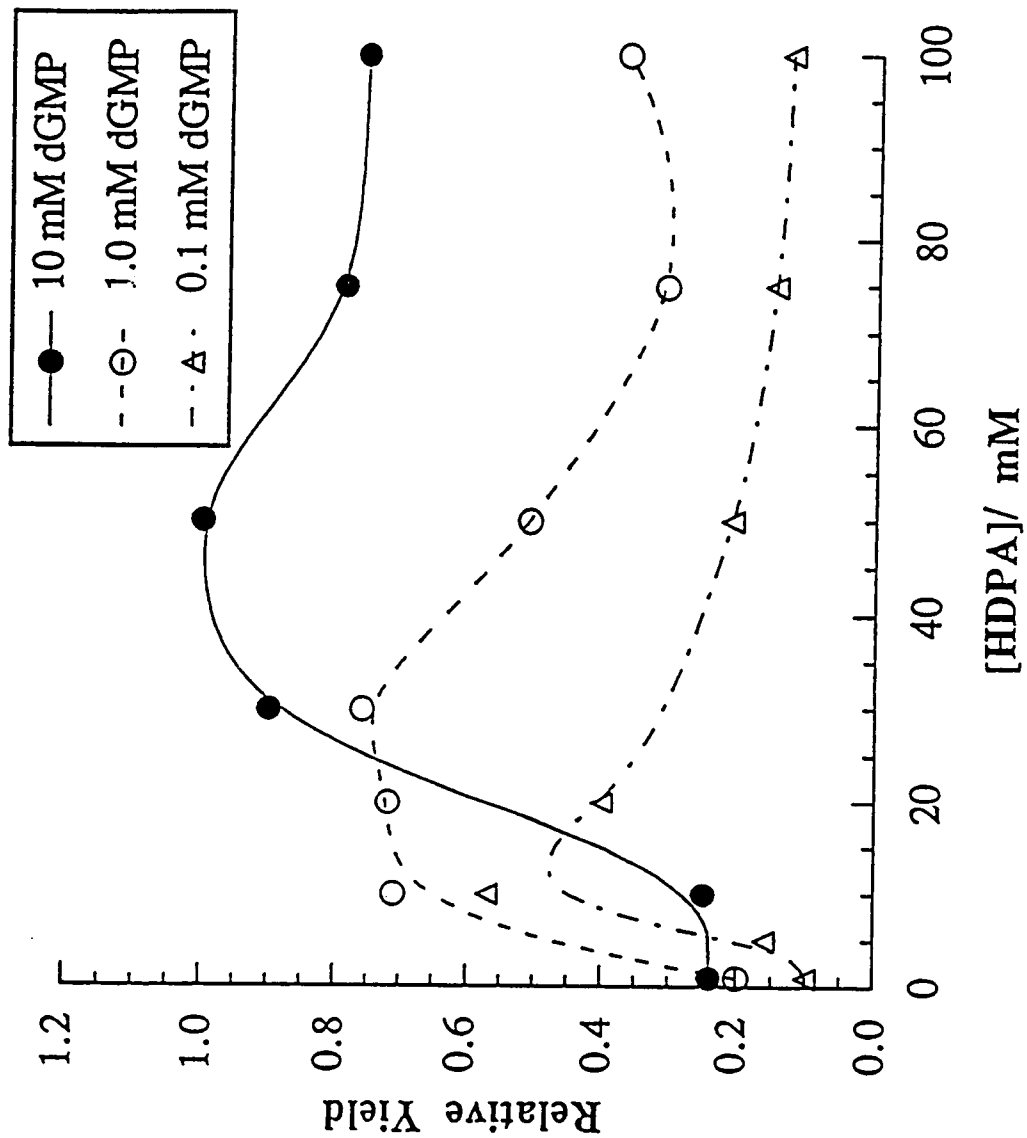

Figure 3.19. Femtomole detection of dAMP by LSIMS/TOFMS. a) 15 pmoles in glycerol and b) 4 fmoles in 10 mM HDPAc/glycerol.

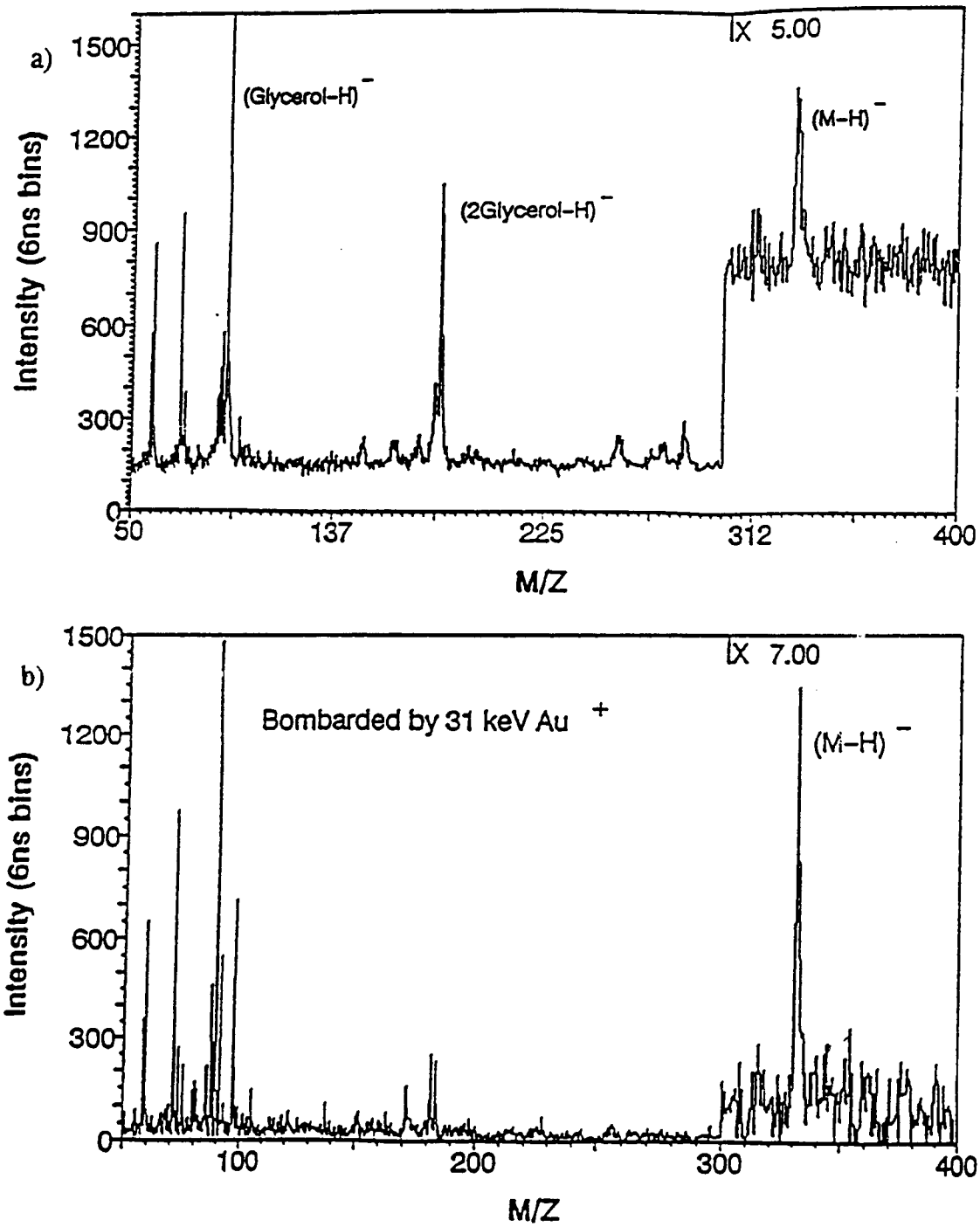

Figure 3.20 Femtomole detection of dGMP by LSIMS/TOFMS. a) 30 pmoles in glycerol and b) 5 fmoles in 10 mM HDPAc/glycerol.

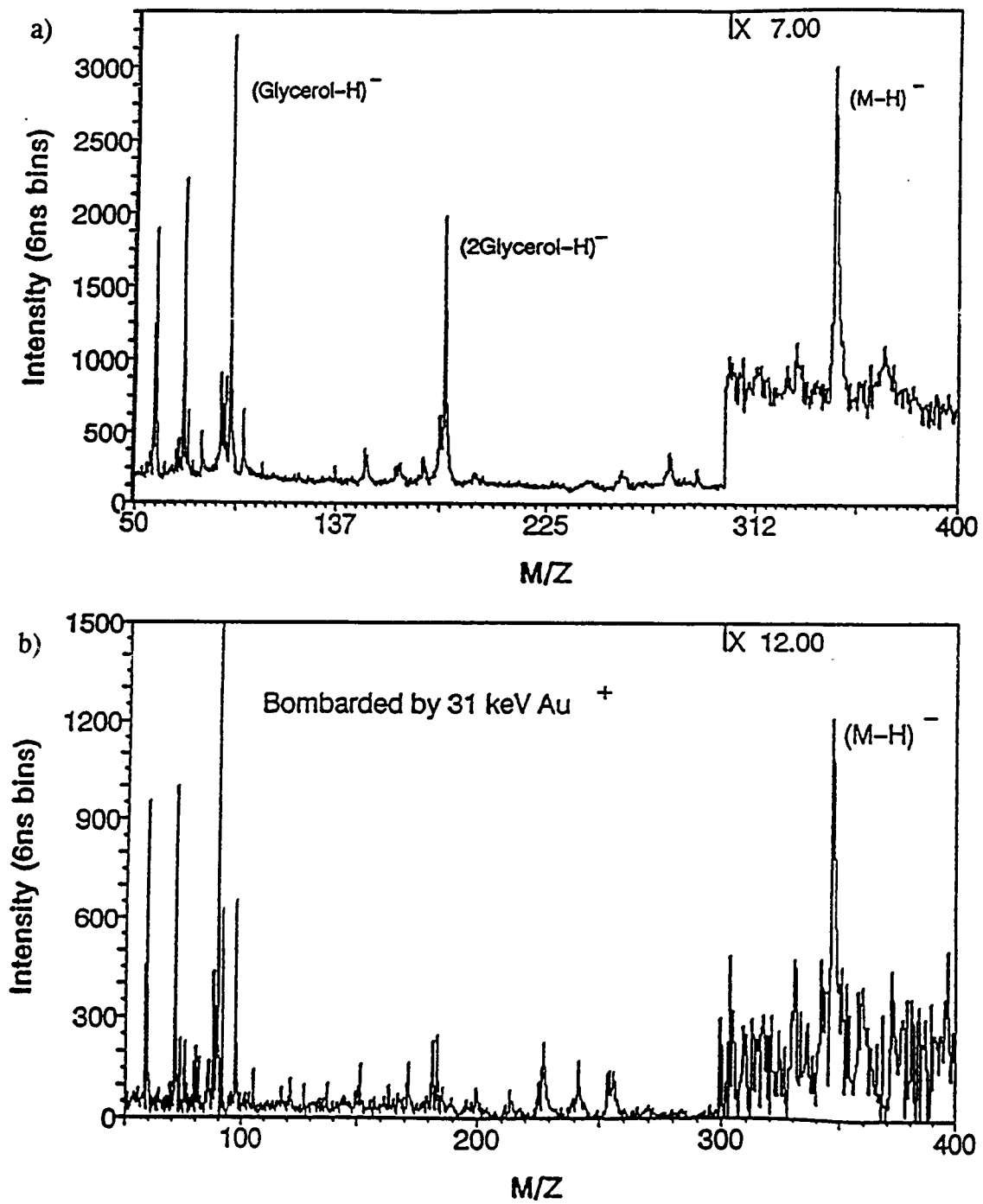

3.4 Anionic surfactant

Ligon and Dorn suggested that a highly acidic surfactant could be used to induce a charge in an ionizable analyte species and, subsequently, ion-pair with the charged species, thus enhancing the analyte's surface activity. The compound suggested was a C_{18}-alkylperfluoroglutaric acid.[36] Studies of this compound on the sensitivity of deoxyadenosine in LSIMS indicated that the effect was similar to that of other acids with little surface activity. None of the dramatic effects observed on nucleotides in the presence of HDPAc were apparent.

3.5 Adducted nucleotides

The N^2-benzo[a]pyrene adduct of deoxyguanosine-5'-monophosphate was analyzed in the absence and presence of 5×10^{-3} M HDPAc in glycerol on the Kratos MS-50 in negative ion mode LSIMS. The resulting mass spectra are shown in figure 3.21. In glycerol alone, a 10^{-4} M solution of the analyte produces a signal-to-background ratio of less than two for m/z 648 which corresponds to the $(M-H)^-$ ion of the adducted nucleotide. In the presence of HDPAc, the matrix peaks are suppressed and m/z 648 has a signal-to-background ratio of 6 from a 5×10^{-5} M solution of adduct. Giving approximately a 10 fold increase in sensitivity. The amount of adducted nucleotide loaded onto the probe was 100 pmoles.

Figure 3.21. Sensitivity enhancement of dGMP-B[a]PDE adduct. a) 10^{-4} M in glycerol and b) 5 x 10^{-5} M in 10^{-3} M HDPAc/glycerol.

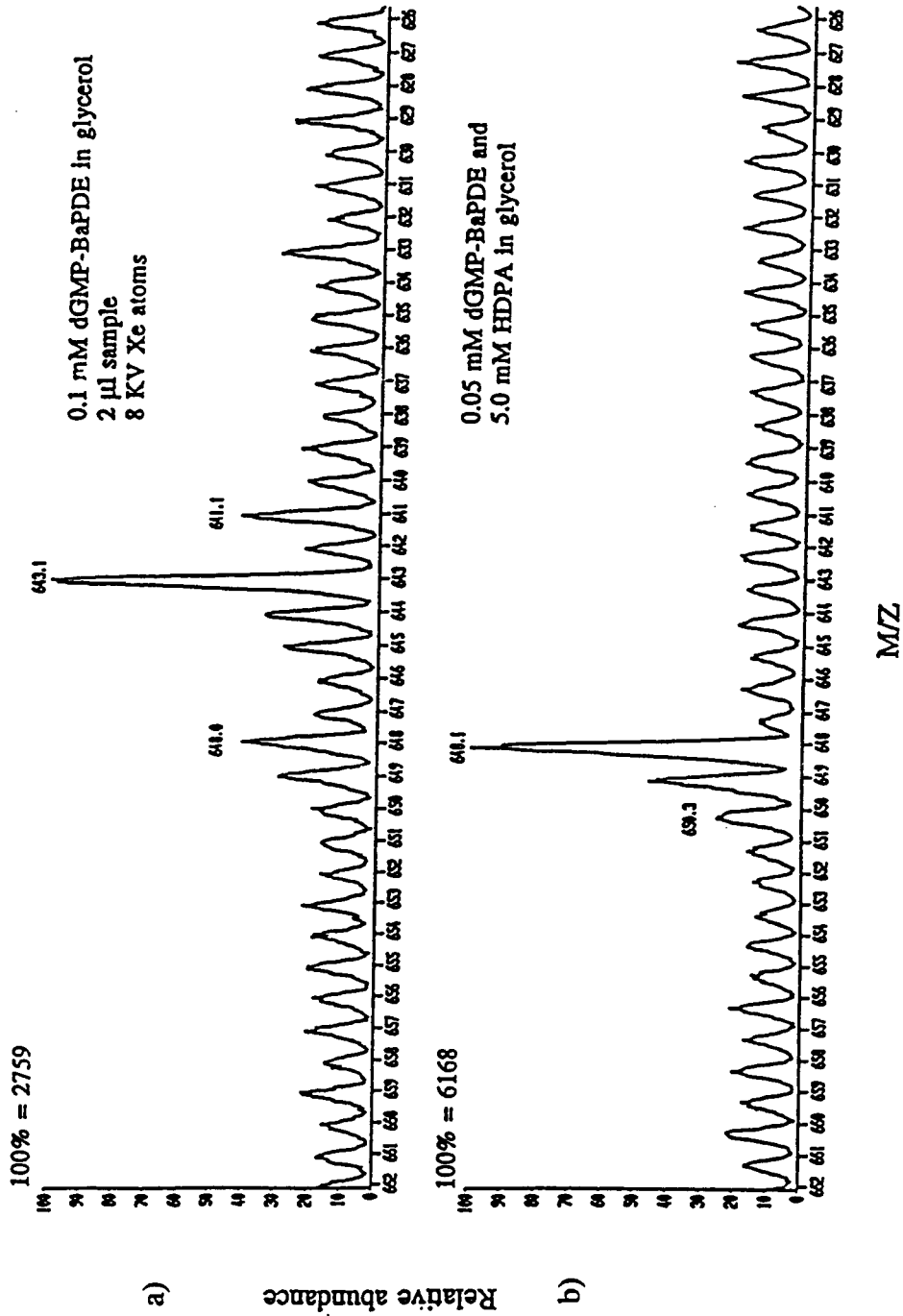

Chapter 4

Discussion

4.1 Qualitative aspects of sensitivity enhancement

The presence of the surfactant enhances the sensitivity toward the ionic analyte by two mechanisms. The first and minor mechanism is the suppression effect. This effect lowers the background used to calculate the signal-to-background ratio. The surfactant displaces the matrix at the surface of the target decreasing its exposure to the incoming particle and its ability to escape the surface, thereby preventing significant amounts of the matrix from being sputtered. The second and major mechanism is the increase in surface (or near surface) concentration of the ionic analyte due to its ion pairing with surface adsorbed surfactant. It is this mechanism that we are attempting to elucidate beyond a mere qualitative understanding so that this phenomenon's general applicability be determined and its utilization can be made more effective.

A conceptual view of the phenomenon is illustrated in figure 4.1. For our purposes, the near surface region is defined as the volume effectively sputtered in the particle induced desorption experiment. In general, a non-surface active solute in a matrix at a specific bulk concentration has a near surface concentration prescribed by the random distribution of solute throughout the solution volume. Surface active molecules, on the other hand, preferentially occupy the surface region to an extent

Figure 4.1. Schematic of surfactant action in glycerol solutions.

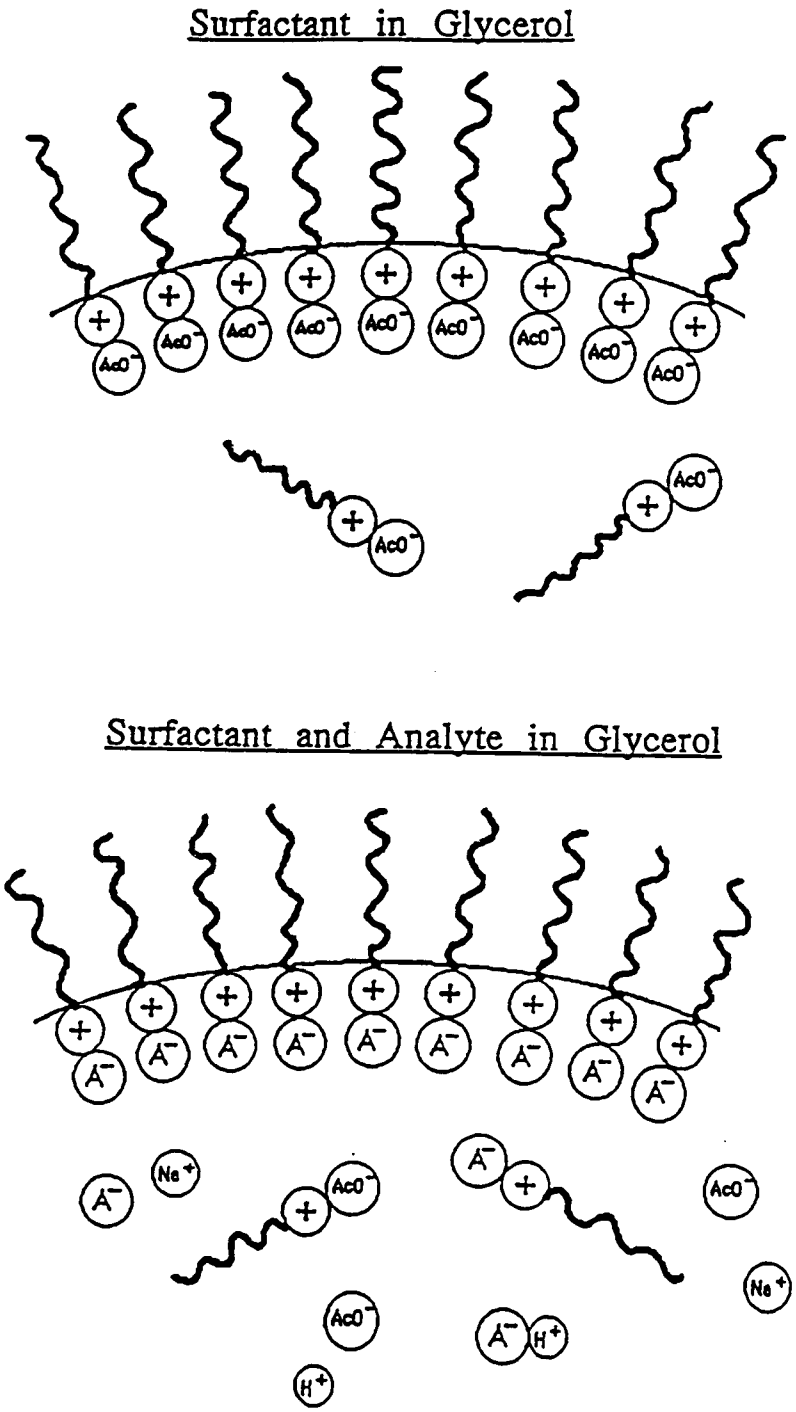

significantly greater than expected from the bulk concentration. Sampling the surface of a solution containing a surface active species would yield a greater number of solute molecules than would be obtained from the solution of a non-surface active species with the same bulk concentration. When an ionic surfactant is employed, a counterion accompanies it to the surface to maintain electric neutrality. Any ion of appropriate charge in the solution may act as the counterion. Thus a charged analyte may be enriched at the surface by the presence of an ionic surfactant of opposite charge.

Ideally, the surfactant and analyte would be put into solution as a single salt for optimum analyte surface concentration. In practice, this would require significant foreknowledge as to the identity and quantity of the species to be analyzed. More realistically, the analyte is present in solution as an acid or common salt. The surfactant must then necessarily be added with its own counterion. This leads to a four component equilibrium in solution (neglecting solvent) in addition to bulk-surface equilibrium. Intuitively, the choice of the surfactant's counterion should be such that it will not compete effectively with the analyte in ion-pairing with the surfactant. In the present study, acetate ion was chosen for precisely this reason.

It must be remembered that during particle bombardment, the solution is not at equilibrium and, consequently, that equilibration of the surface concentration is unlikely to be achieved. As the limiting case of particle bombardment with infinitesimally low primary particle flux density is approached, there is ample time between individual

sputtering events, i.e. the impact of individual primary particles, for complete replenishment of the surface and equilibrium surface concentrations will be approached. As the limiting case of infinitely high flux density is approached sputtering occurs without surface replenishment and surface concentrations would quickly decrease to those representative of the bulk. In a typical particle induced desorption experiment, a steady state lying somewhere between these limiting cases should exist. Therefore, it would seem both reasonable and useful to use chemical equilibria theory to estimate a first approximation to the surface concentration of the analyte species in the presence of surfactant. Ideally, such an approach would enable us to design appropriate surfactant systems for a wide range of ionic analytes prior to entering the laboratory.

4.2 The Langmuir isotherm

The primary equilibrium of interest is the partition of an analyte, A, between the bulk phase and the near surface region. This can be represented by the equation

$$G_S + A_B \rightleftarrows A_S + G_B \qquad (4\text{-}1)$$

where G represents the solvent - in our case, glycerol - and the subscripts S and B designate species at the surface or in the bulk, respectively. One may, therefore write an equation for the equilibrium constant, K′, in the usual manner.

$$K' = [A]_S[G]_B/[G]_S[A]_B. \qquad (4\text{-}2)$$

In dilute solutions, concentrations may be used instead of activities. Since, under dilute conditions the bulk concentration of the solvent is essentially constant, we take K to equal $K'/[G]_B$ and

$$K = [A]_S/[G]_S[A]_B. \qquad (4\text{-}3)$$

Assuming the two dimensional surface solution to be ideal allows surface concentration to be replaced with mole fraction at the surface, x_S. Making this substitution gives

$$K = x^A_S/x^G_S[A]_B \qquad (4\text{-}4)$$

Since this is a two component system, $x^G_S + x^A_S = 1$, and the equation can be written

$$K = x^A_S/(1 - x^A_S)[A]_B. \qquad (4\text{-}5)$$

Solving equation 4-5 for x^A_S yields

$$x^A_S = K[A]_B/(K[A]_B + 1). \qquad (4\text{-}6)$$

Finally, assuming that solvent and solute occupy the same area per molecule, equation 4-6 is equivalent to

$$\theta_A = K[A]_B/(K[A]_B + 1), \qquad (4\text{-}7)$$

where θ_A is the fraction of the surface occupied by the analyte.

Equation 4-7 is in the form of a Langmuir adsorption isotherm.[29] At infinite dilution the equation reduces to

$$\theta_A = K[A]_B. \qquad (4\text{-}8)$$

Therefore, a plot of θ_A versus analyte bulk concentration (figure 4.2) would have an initial slope of K. Alternately, from equation 4-7, it can be seen that at $\theta_A = 0.5$, then

$$K = 1/[A]_B. \qquad (4\text{-}9)$$

In one of our mass spectrometry experiments, the condition indicated by equation 4-9 corresponds to the surfactant-analyte ion pair concentration that produces a surfactant signal equal to 1/2 of the value it asymptotically approaches at high surfactant concentration, or to a matrix signal that is 50% suppressed from its magnitude in the absence of surfactant.

Figure 4.2. The Langmuir isotherm.

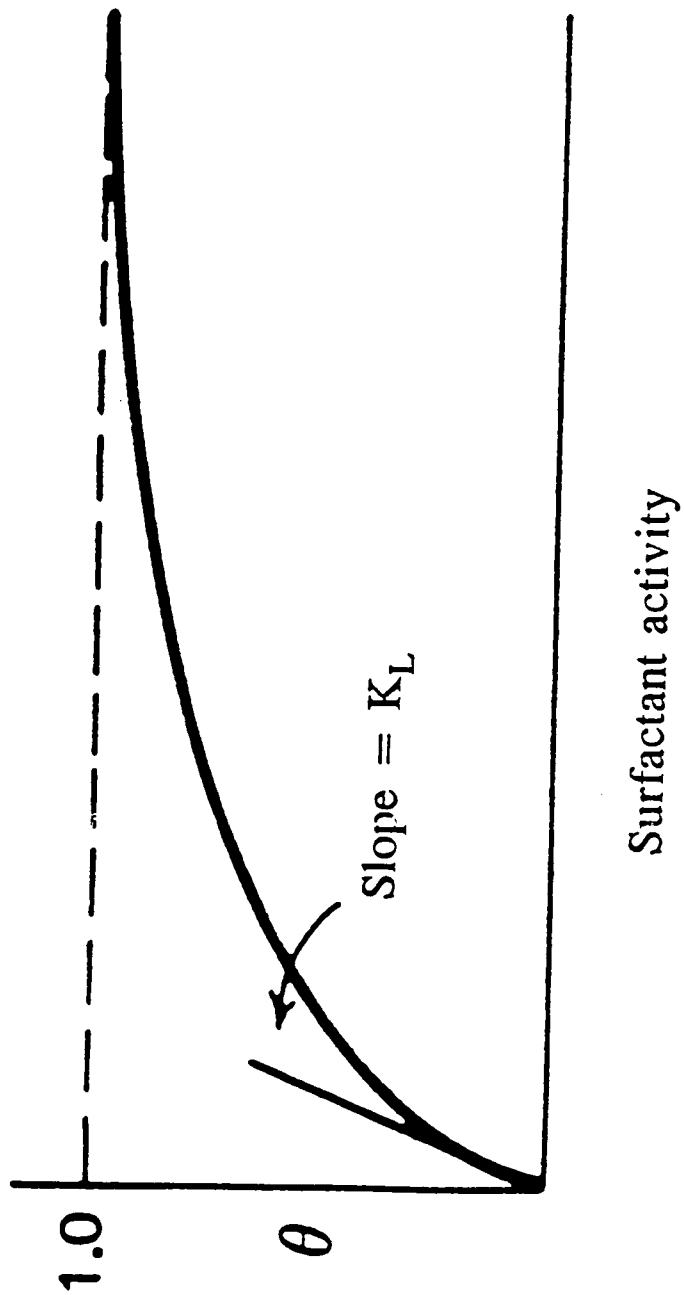

4.3 Ionic equilibria

In addition to the surface-bulk equilibrium, ion-pairs necessarily exhibit finite ionization in polar solvents. If we consider the ion pairing of the surfactant of interest, HDP^+, and the nucleotide anion, N^-, the reaction would be represented by

$$HDPN \rightleftarrows HDP^+ + N^-. \qquad (4\text{-}10)$$

The equilibrium constant is then

$$K_1 = [HDP^+][N^-]/[HDPN] \qquad (4\text{-}11)$$

Solving for the ion pair concentration gives us

$$[HDPN] = (1/K_1)[HDP^+][N^-]. \qquad (4\text{-}12)$$

Recasting equation 4-3 such that our ion pair is species A, and using the subscript L to distinguish the Langmuir equilibrium constant, we obtain

$$K_L = [HDPN]_S/[G]_S[HDPN]_B. \qquad (4\text{-}13)$$

Using equation 4-12 to substitute for $[HDPN]_B$ and solving for $[HDPN]_S$ yields

$$[HDPN]_S = K_L(1/K_1)[G]_S[HDP^+]_B[N^-]_B. \qquad (4\text{-}14)$$

In this work, HDP^+ is added to the sample solutions as the acetate salt, HDPAc. Therefore, its ionization equilibrium must be considered:

$$HDPAc \rightleftarrows HDP^+ + Ac^-. \qquad (4\text{-}15)$$

The nucleotide is usually present as the acid, therefore,

$$HdAMP \rightleftarrows H^+ + dAMP^-, \qquad (4\text{-}16)$$

and

$$HAc \rightleftarrows H^+ + Ac^-. \qquad (4\text{-}17)$$

Finally, each species present has a finite surface concentration based solely on the statistical distribution of solute throughout the solution volume. Therefore, equation 4-2 could be written for each. The value of K' in the case of non-surface active species would be unity if we assume the concentrations in the near surface region to be the same as those of the bulk. Since we incorporated $[G]_B$ into the constant K, $K = 1/[G]_B$.

At this point, there are five equilibria that, because they are coupled, must be simultaneously satisfied. Speciation may be calculated from equilibria constants and known total component concentrations, i.e. the summed concentrations of all species containing a specific component or, empirically, the amount of each component added to the solution. This is conveniently accomplished using a computer program MICROQL developed by John C. Westall.[56]

4.4 Calculation of equilibrium surface concentrations

Figure 4.3 is a MICROQL input matrix for a simplified two surfactant system. A component, X, is used to designate a surface adsorption site. In theory, free X is equivalent to G_S as described above since all surface sites are necessarily occupied by either a solute or the solvent, glycerol. The total concentration of X is calculated from the cross sectional area of the surfactant, σ, (all species are assumed to have the same cross-sectional area when occupying a surface site), and the surface-area-to-volume ratio, A_S/V, of the sample solution on the mass spectrometer probe and is expressed in units of molarity.

$$T_X = (A_S/V)/(\sigma N_A), \qquad (4\text{-}18)$$

where N_A is Avogadro's number. For the probe geometry of the Kratos MS-50, the total concentration of surface sites in 2 μL of sample solution was estimated to be 10^{-6} M.

4.4.1 Estimation of equilibrium constants

In order to obtain K_L's for the two surfactant ion pairs studied, HDPAc and HDPdAMP, the ion signals for the glycerol trimer and HDP^+ were plotted versus surfactant salt concentration (figure 4.4). The glycerol trimer was monitored because of its proximity to the HDP^+ ion. Barber has reported that the suppression of the glycerol trimer corresponds well with surface coverage.[35] It was assumed that, at the concentration for which $\theta_A = \theta_X = 0.5$, the ionized portion of the salt would be negligible when no other counterions are present and, therefore, the total concentration could be used with minimal error in equation 4-9. The equilibrium constant was estimated from the suppression of the glycerol ion signal rather than the increase of the surfactant ion signal because the latter data were more erratic. This fluctuation in the surfactant ion signal may be caused by transport of micelles to the surface where they rapidly dissociate and supersaturate the surface with surfactant; Ligon has postulated such events.[30]

Dissociation constant, K_d, for HDPAc was initially estimated using FITEQL.[56] a computer program that accepts serial data, such as that plotted in figure 4.4, and

Figure 4.3. MICROQL input for ideal two surfactant model.

```
I. Components
   ##    Name      log X     Total []     TYPE
   1     HDPN      0.00      0.00         Total
   2     HDPAc     0.00      0.00         Total
   3     X         0         0            Total

II. Species
##  Name     log K     HDPN     HDPAc     X
1   HDPN     0.00      1        0         0
2   HDPAc    0.00      0        1         0
3   X        0.00      0        0         1
4   XHDPN    3.00      1        0         1
5   XHDPAc   3.00      0        1         1
```

Known
Known
Known

Figure 4.4. Glycerol trimer and HDP^+ ion signals versus HDPAc concentration.

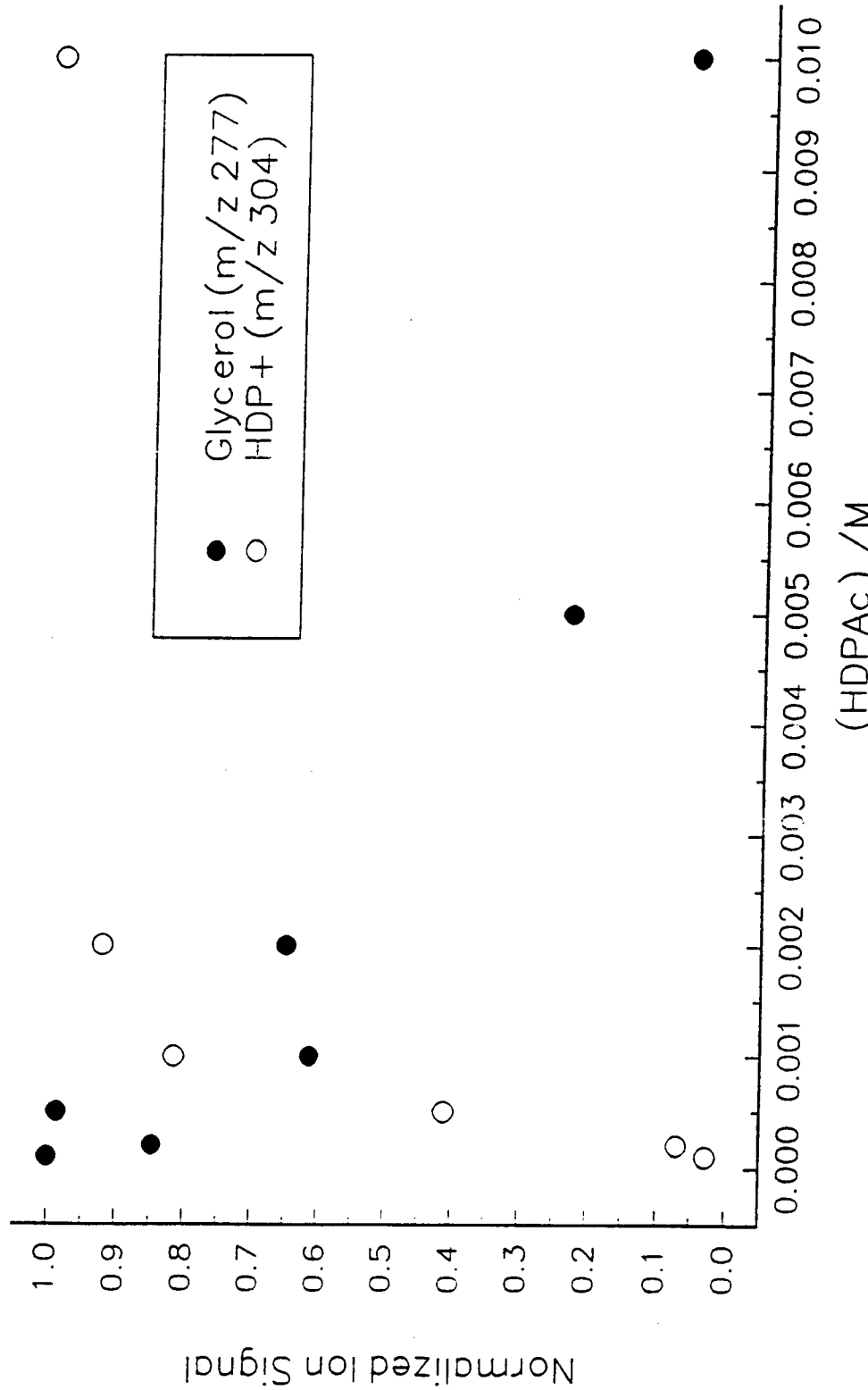

extracts one or more equilibrium constant through an iterative optimization process. The dissociation constant for HDPN was estimated relative to that for HDPAc by correlating the dissociation constants with ion exchange relative selectivities of strong basic anion exchangers for acetate and phosphates.[57]

Finally, estimates of acidity constants for HdAMP and HAc in glycerol were based on the corresponding values for aqueous systems found in the literature and, using Caprioli's observations,[58] corrected for the difference in dielectric strength. Caprioli found apparent pK_a's for a number of different organic acids to change nearly linearly in water/glycerol systems with percent glycerol in the solvent; extrapolating that data back to pure water provided good agreement with published values determined by potentiometric means. To serve our purposes, we have extrapolated the data to 100% glycerol.

4.4.2 Comparison of calculated equilibria to mass spectral data

Figure 4.3 shows the MICROQL input matrix for a system consisting of surface active species HDPN and HDPAc, and figure 4.5 shows the surface concentration of HDPN computed from this data by the program plotted as a function of total surfactant concentration. In this model, all ionization equilibria are neglected in order to observe the competition of the two species at the surface only. The surface concentration corresponds to the dGMP signal as plotted in figure 3.11. The total surfactant concentration on the horizontal axis is the sum of the HDPN and HDPAc concentrations.

Figure 4.5. Calculated nucleotide surface concentration from idealized model.

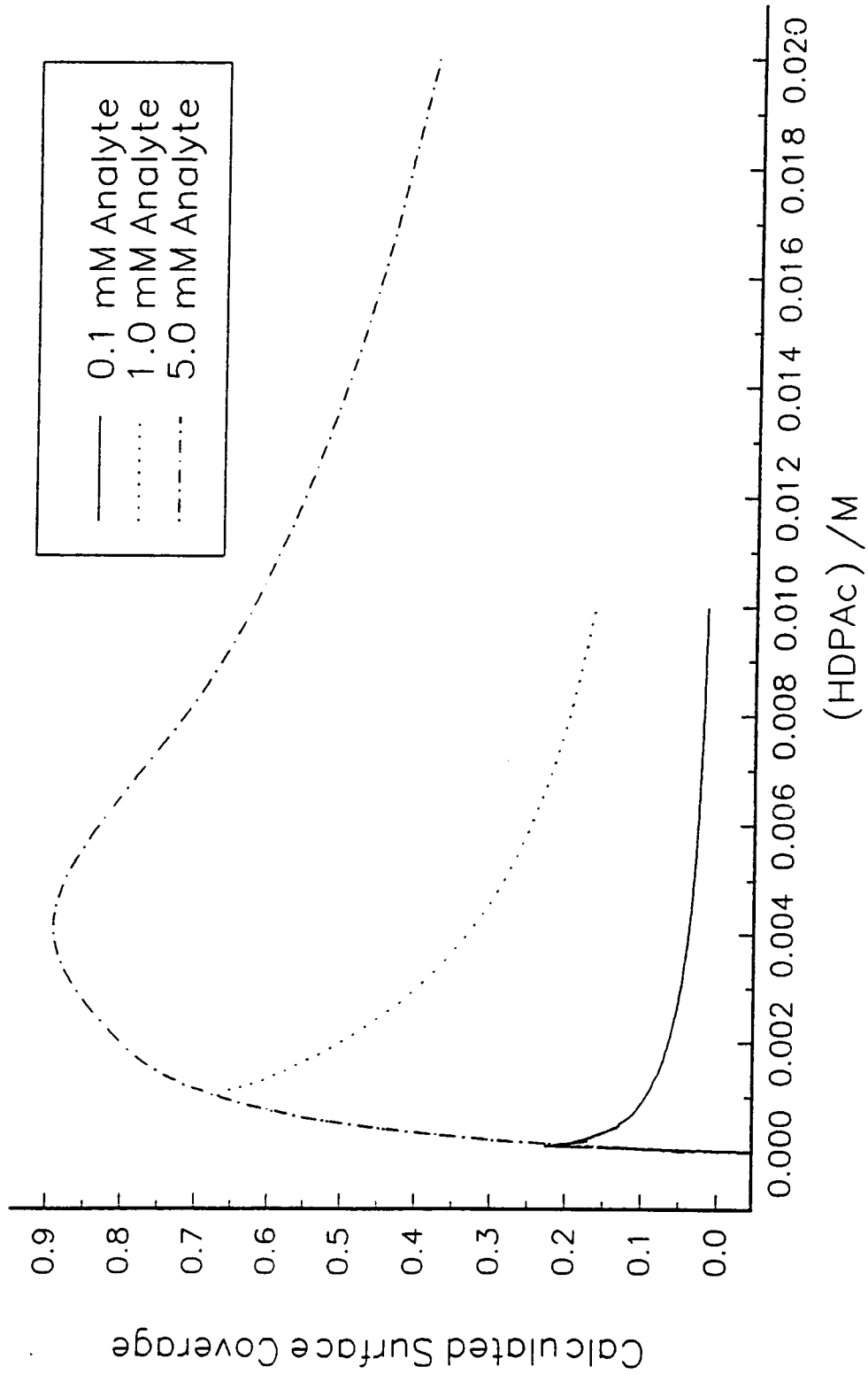

To generate the plot in figure 4.5 it was assumed that the analyte, N, quantitatively substitutes for acetate as counterion to the surfactant and that the resulting ion pair has negligible dissociation in solution. Once the N in solution has been exhausted the acetate pairs quantitatively with the surfactant. This idealized model accounts for the basic features exhibited by the experimental data displayed in figures 3.11, 17, 18. The initial slope of both experimental and theoretical curves is nearly linear for all three concentrations of analyte shown, and the maxima of both experimental and theoretical curves shift to higher surfactant concentrations at higher analyte concentrations. The maxima in these curves correspond to the concentration of surfactant that produces the highest surface excess of analyte (actually analyte-surfactant ion pair) for a given analyte concentration. In the idealized plot, the position of this optimum surfactant concentration corresponds quantitatively to the analyte concentration, whereas in the experimental data the position of the optimum surfactant concentration is less sensitive to changes in the analyte concentration. This model shows clearly, however, that the general form of the experimental data set may be explained on the basis of a competition between surface active species. Above the optimum concentration of surfactant, the acetate-surfactant ion pair begins to displace the analyte from the surface. If both ion pairs have the same affinity for the surface, the data should follow a simple dilution curve. At concentrations below the optimum the curve is identical with the adsorption isotherm of the analyte-surfactant ion pair.

If the assumption of negligible dissociation of the analyte-surfactant ion pair is relaxed, the resulting dissociation of the ion pairs produces a coupled equilibrium wherein the acetate competes with the analyte for surfactant ions in solution. The effect of this is illustrated in figure 4.6. The optimum surfactant concentration is no longer identical to the analyte concentration, and its sensitivity to analyte concentration is reduced, additionally the peak is not as sharp. The maximum analyte surface concentration is necessarily reduced since the concentration of ion pairs in solution is decreased by dissociation.

Finally, if the acid-base equilibria due to the presence of the analyte in its acid form are invoked by using the input matrix in figure 4.7, the curves in figure 4.8 result. Also shown in figure 4.8 are the mass spectral dGMP responses to increasing surfactant concentration. The data for the 10^{-3} and 10^{-4} M dGMP series are almost in quantitative agreement with the calculated values. The model, however, overestimates dGMP signal above the optimum surfactant concentration for the 10^{-2} M dGMP series. Whether this represents a real effect on the actual analyte surface concentration, or a characteristic of the ionization process is unknown at this time. It is possible that at high surface concentrations the analyte molecules are more likely to be sputtered in groups with surfactant and other analyte molecules. Some such clusters were observed in the plasma desorption spectra. The molecular ion signal could be reduced relative to the actual surface concentration if such clusters accounted for a significant fraction of the total analyte sputtered at higher concentrations.

Figure 4.6. Calculated nucleotide surface concentration including ion pair dissociation.

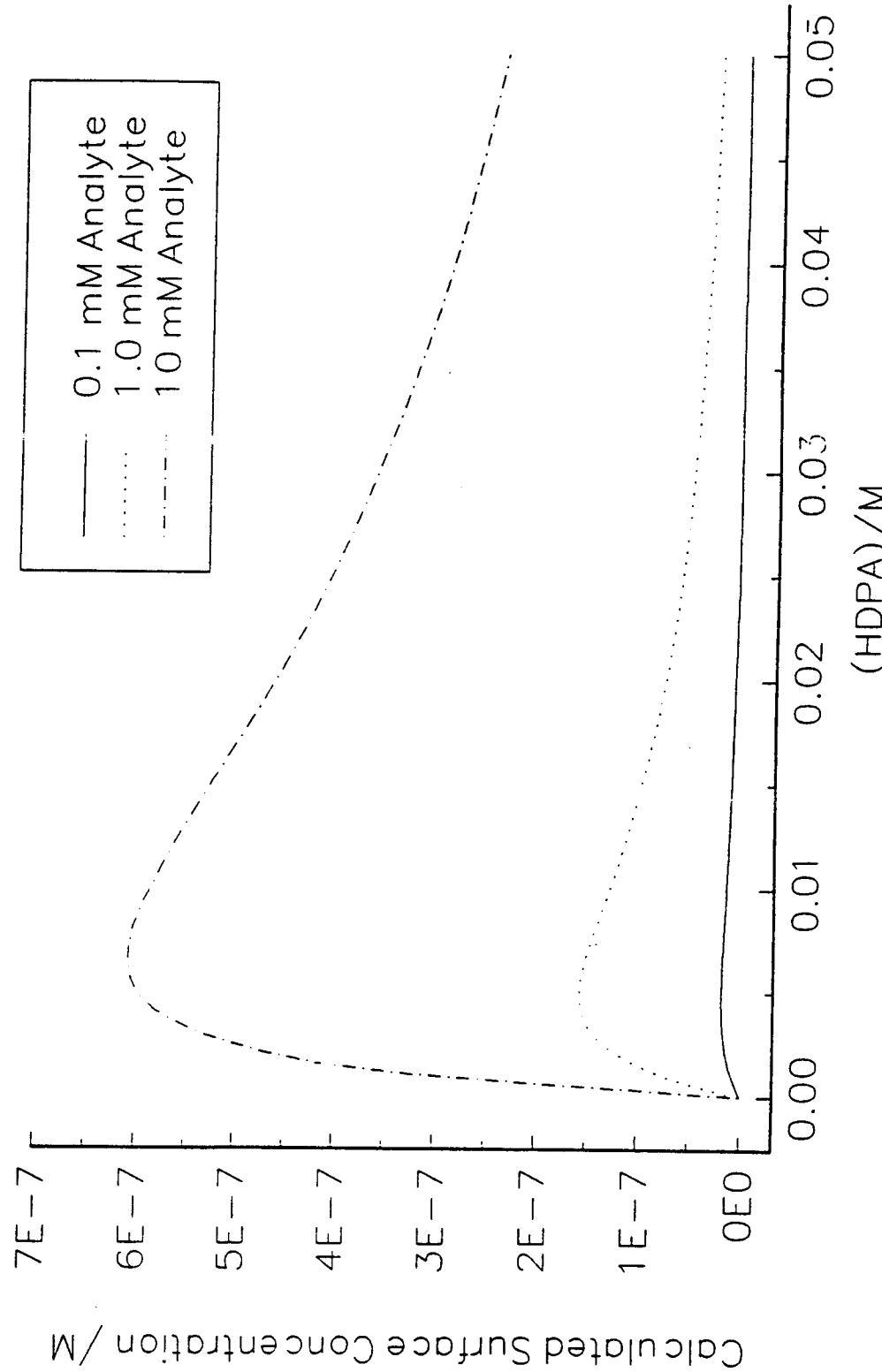

Figure 4.7. MICROQL matrix for a five component equilibrium.

I. Components

##	Name	log X	Total [ ]	TYPE	
1	HDP+	-6.000	5.000D-02	Total	Known
2	N-	-6.000	1.000D-04	Total	Known
3	Ac-	-6.000	5.000D-02	Total	Known
4	H+	-6.000	1.000D-04	Total	Known
5	X	-6.000	1.000D-06	Total	Known

II. Species

##	Name	log K	HDP+	N-	Ac-	H+	X
1	HDP+	0.000	1	0	0	0	0
2	N-	0.000	0	1	0	0	0
3	Ac-	0.000	0	0	1	0	0
4	H=	0.000	0	0	0	1	0
5	X	0.000	0	0	0	0	1
6	HDPN	2.000	1	1	0	0	0
7	HDPAc	1.500	1	0	1	0	0
8	HN	7.000	0	1	0	1	0
9	HAc	5.300	0	0	1	1	0
10	XHN	5.85	0	1	0	1	1
11	XHAc	4.15	0	0	1	1	1
12	XHDPN	5.000	1	1	0	0	1
13	XHDPAc	4.500	1	0	1	0	1

Figure 4.8. Comparison of calculated nucleotide surface concentration and dGMP mass spectral data.

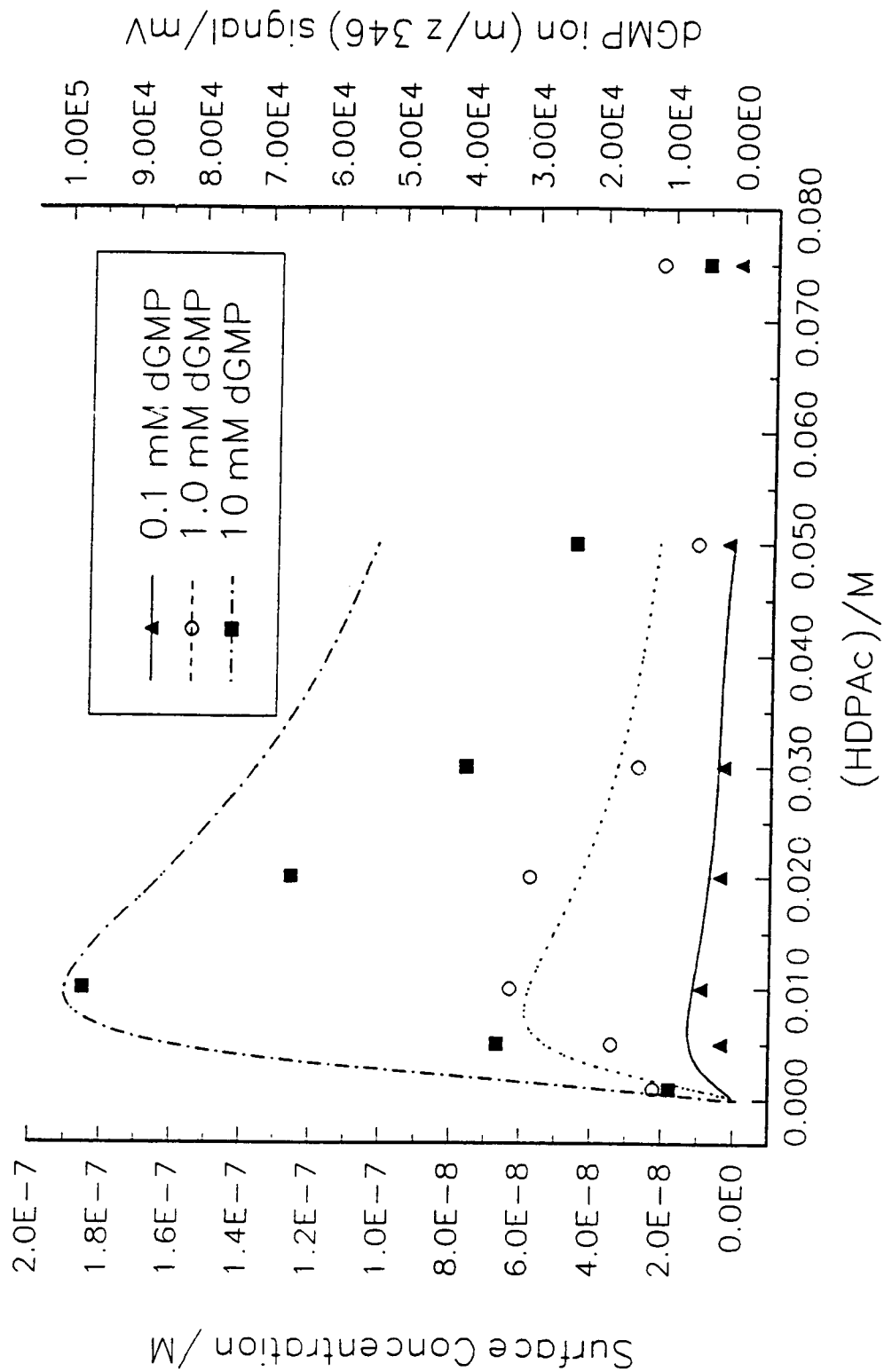

Similar agreement is observed in figure 4.9 between the ATP mass spectral data and the calculated curves from figure 4.6. The acid equilibrium is ignored since the nucleotide is introduced into solution as a salt. Again the model overestimates the signal at higher surfactant concentrations. Still, the major features of the data are described by the model.

To predict absolute sensitivity enhancement, a value for the surface concentration of a non-surface-active analyte may be calculated assuming the mole fraction of analyte in the surface layer is the same as that in the bulk. The molarity of pure glycerol is 14.1 M. So an analyte having a bulk concentration of 0.01 M is in solution at a mole fraction of 7.1×10^{-3} and would have a concentration in the surface layer of 7.1×10^{-10} M. Analytes in solution at 10^{-3} M and 10^{-4} M would have surface concentrations in our system of 7.1×10^{-11} M and 7.1×10^{-12} M respectively. The predicted maximum sensitivity gain for the model in figure 4.8 is plotted as a function of analyte concentration in figure 4.10. Our observed sensitivity enhancement for mononucleotides was on the order of 200 to 1000X.

The greatest source of uncertainty associated with the model presented here is the estimation of the various equilibrium constants. In particular, the dissociation constants of the ion-pairs are not well known. Increasing the dissociation constants has the effect of lowering the maxima and shifting them toward higher surfactant concentrations. This may account for the significant shift in the liquid metal

Figure 4.9 Comparison of calculated surface concentration and ATP mass spectral data.

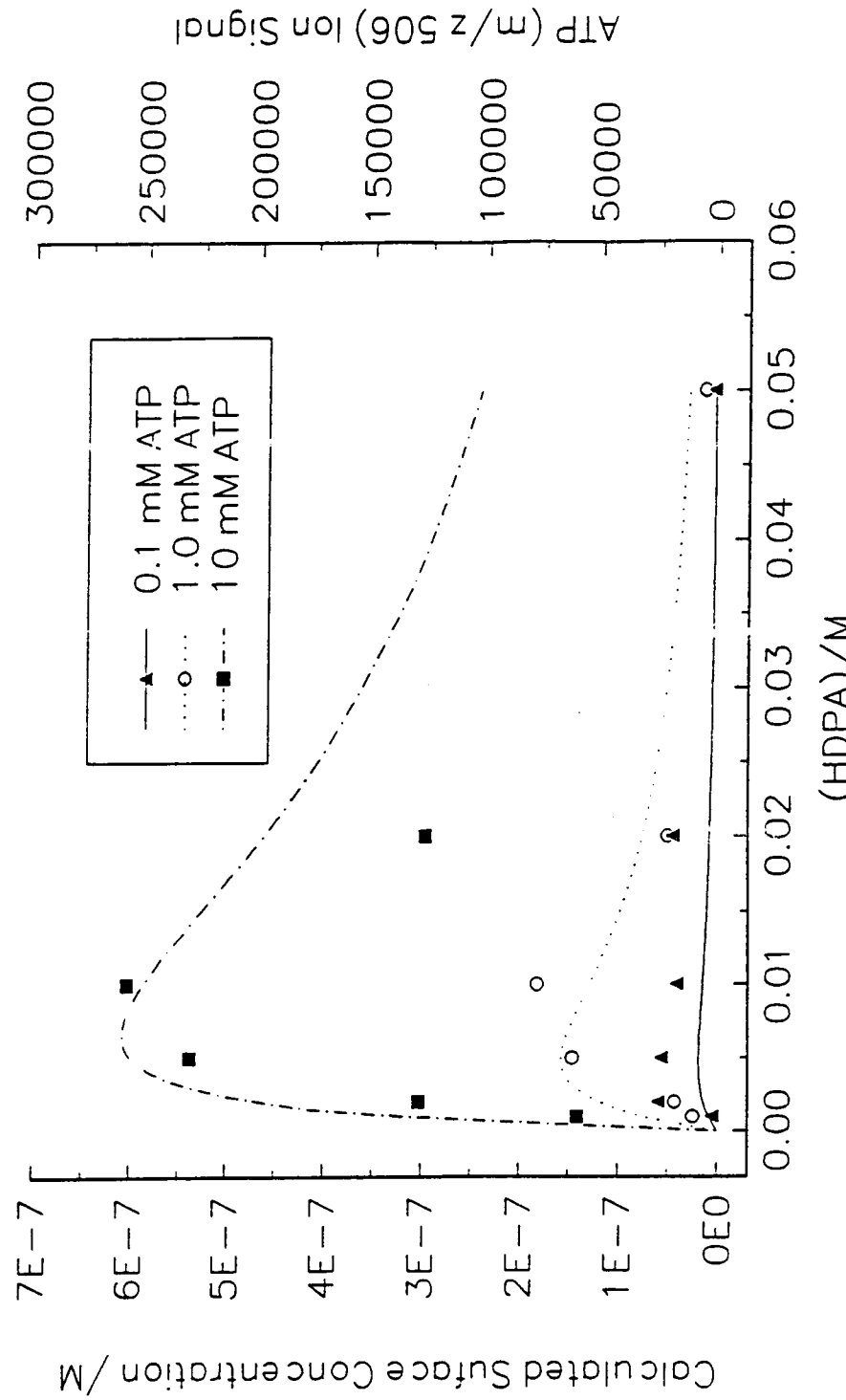

Figure 4.10 Maximum sensitivity enhancement vs. analyte concentration.

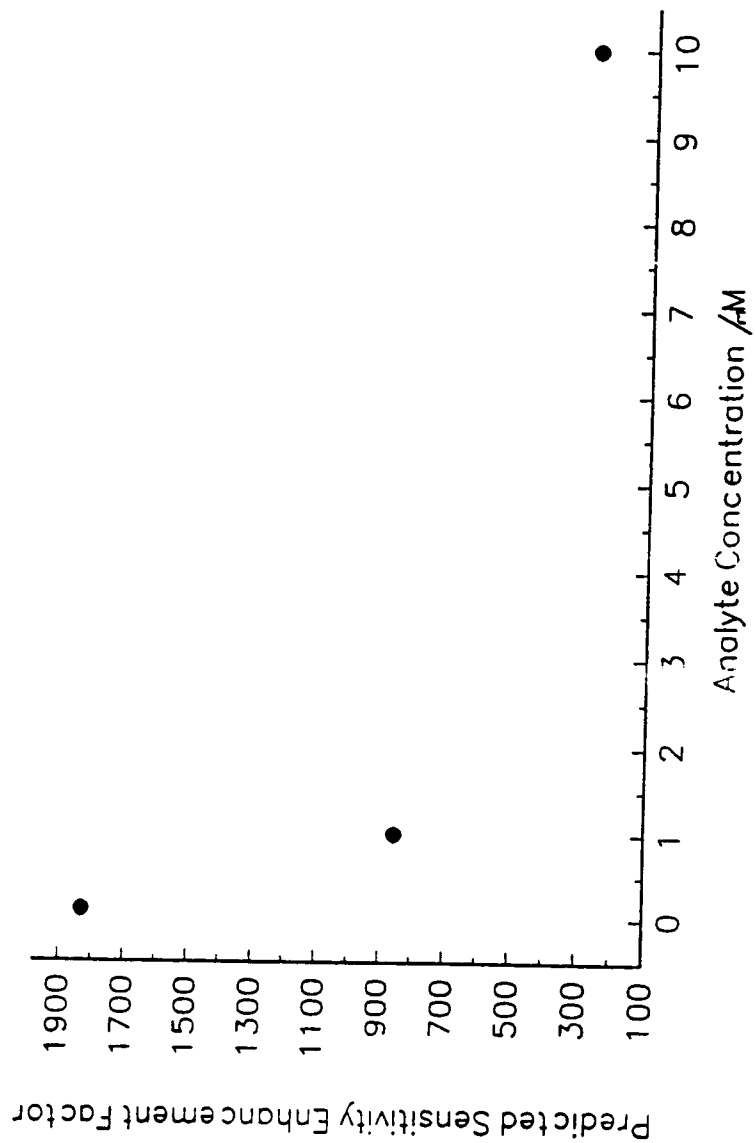

ion source data for dAMP (figure 3.18). Since, in these experiments, the water was not scrupulously removed under vacuum prior to analysis, some water may have remained in the matrix; such excess water would lower the K values for ion-pair formation (increase the dissociation constants), thus, shifting the maxima of resulting curves to higher surfactant concentrations. Additionally, the surface to volume ratio of sample placed on this probe in the liquid metal ion experiments was on the order of 100X greater than that of the conventional LSIMS probe; this would have the effect of significantly increasing the effective concentration of the surface adsorbed species in accordance with equation 4-18.

4.5 Conclusions

The general goal of this study was to investigate particle induced desorption mass spectrometry of nucleotides from liquid matrices. The specific goals were 1) to acquire quasi-equilibrium data that characterizes the equilibrium and steady state conditions prevalent during particle bombardment of a surfactant containing liquid matrix 2) to use classic chemical equilibrium and surface chemical principles to develop a semiquantitative model that identifies the primary chemical features affecting ion emission in particle induced desorption from liquid matrices and that predict the enhancement in sensitivity due to the pairing of an ionic analyte, specifically a nucleotide, and a surfactant, and 3) to apply the knowledge gained to increase the

sensitivity of liquid matrix assisted secondary ion mass spectrometry toward nucleotides, in particular nucleotide-polynuclear aromatic hydrocarbon adducts.

Despite the dynamic nature of the particle induced desorption-ionization technique, quasi-equilibrium data was obtained and a theoretical model that semiquantitatively explains the mass spectral data was developed. While the general applicability of this model has not been conclusively demonstrated, it should be possible, in principle, to adapt it to any agent - not just surfactant - that enhances surface activity of an analyte, e.g. derivatization or hydrophobicity, and for which an equilibrium reaction expression can be written.

The results of this study imply that mass spectrometry can be useful as a tool for the study of both surface and solution chemistry. Caprioli has already demonstrated the ability of LSIMS to experimentally determine pK_a's of weak acids.[58] Similarly, experiments could be designed to determine equilibrium constants of a variety of systems in terms of the parameters described in the previous section. The ability to measure numerous species discretely and simultaneously could make it an ideal complement to established techniques, such as potentiometry.

In terms of the practical goal of increasing the sensitivity of LSIMS to nucleotide analysis, low femtomole detection of these species was achieved by the combination of the surfactant ion-pairing effect and a high transmission, low sample

utilization, time-of-flight mass spectrometer. A sensitivity enhancement on the order of 10X was observed for the benzo[a]pyrene adduct at the N^2 position of deoxyguanosine-5'-monophosphate at 10^{-4} M in glycerol/surfactant. Further enhancement may be possible in the case of the adducted nucleotide. The studies were hampered by the difficulty in obtaining quantities of the adduct that were sufficiently free of buffer salts that complicate the ion-pairing equilibria.

Bibliography

1. M. Barber, R. S. Bordoli, R. D. Sedgwick, A. N. Taylor, (1981) *J. Chem. Soc. Chem. Commun*, 325.

2. D. F. Torgerson, R. P. Skrowronski, R. D. Macfarlane, (1974) *Biochem. Biophys. Res. Commun.* **60,** 616.

3. A. Benninghoven, D. Jaspers, W. Sichtermann, (1976) *Appl. Phys.* **11,** 35.

4. W. Aberth, K. M. Straub, A. L. Burlingame, (1982) *Anal. Chem.* **54,** 2089.

5. R. G. Cooks, S. J. Pachuta, (1987) *Chem. Rev.* **87,** 647-699.

6. J. L. Gower, (1985) *Biomedical Mass Spectrometry,* **12**(5), 191-196.

7. K. D. Cook, P. J. Todd, D. H. Friar, (1989) *Biomed. Environ. Mass Spectrom.* **18,** 492-497.

8. C. Fenselau, R. J. Cotter, (1987) *Chem. Rev.* **87,** 501-512.

9. W. V. Ligon, S. B. Dorn, (1984) *Int. J. Mass Spectrom. Ion Proc.* **57,** 75.

10. B. Divisia-Bohorn, G. Kyriakakou, J. Ulrich, (1985) *Org. Mass Spectrom.* **20,** 463-466.

11. M. E. Rose, M. L. Prescott, M. H. Wiley, I. J. Galpin, (1984) *Biomedical Mass Spectrometry,* **11,** 10-23.

12. K. W. S. Chan, K. D. Cook, (1983) *Anal. Chem.* **55,** 1422-1424.

13. C. Fenselau, (1984) *J. Nat. Prod.* **47,** 215-225.

14. R. L. Cerny, M. L. Gross, (1985) *Anal. Chem.* **57,** 1160-1163.

15. F. H. Field, (1982) *J. Phys. Chem.* **86**(26), 5115.

16. J. Lindhard, (1964) "Thomas-Fermi Approach and Similarity in Atomic Collisions," NAS-NRC publ. 1133.1.

17. W. D. Wilson, L. G. Haggmark, J. P. Bierack, (1977) *Phys. Rev.* **B15,** 2458.

18. J. F. Ziegler in *Ion implantation: Science and Technology,* J. F. Ziegler (Ed.), Academic Press Inc. 1984, p. 51.

19. P. Sigmund, (1969) *Phys. Rev.* **184,** 383.

20. C. T. Reimann, Theoretical models for sputtering and desorption of large bio-organic molecules under collisional and electronic excitation by ion impact, *Nucl. Instrum. Methods*, in press.

21. D. Fenyö, R. E. Johnson, (1992) *Phys. Rev.* **B46,** 5090.

22. L. R. Schronk, R. J. Cotter, (1986) *Biomed. Environ. Mass Spectrom.* **13,** 395-400.

23. J. Sunner, R. Kalatunga, P. Kebarle, (1986) *Anal. Chem.* **58,** 1312-1316.

24. B. D. Musselman, J. T. Watson, C. K. Chang, (1986) *Org. Mass Spectrom.* **21,** 215-219.

25. P. J. Gale, B. L. Bentz, B. T. Chait, F. H. Field, R. J. Cotter, (1986) *Anal. Chem.* **58,** 1070-1076.

26. M. L. Dienzer, B. Arbogast, E. P. Stirchak, D. D. Weller, (1990) *Org. Mass Spectrom.* **25,** 219-224.

27. G. Dube, (1984) *Org. Mass Spectrom.* **19,** 242.

28. A. W. Adamson, *Physical Chemistry of Surfaces,* 4th Ed., John Wiley and Sons, New York, 1982.

29. P. C. Hiemenz, *Principles of Colloid and Surface Chemistry,* 2nd Ed., Marcel Dekker, Inc., New York, 1986.

30. W. V. Ligon in *Biological Mass Spectrometry,* A. L. Burlingame and J. A. McCloskey (Eds.) Elsevier Science Publishing B. V., Amsterdam.

31. K. Tajima, M. Muamatsu, T. SaSaki, (1970) *Bulletin of the Chemical Society of Japan,* **43,** 1991-1998.

32. W. V. Ligon, S. B. Dorn, (1986) *Int. J. Mass Spectrom. Ion Proc.* **78,** 99-113.

33. E. Depauw, G. Pelzer, Dao Viet Dung, J. Marien, (1984) *Biochem. Biophys. Res. Commun.* **123,** 27-32.

34. W. V. Ligon, (1985) *Anal. Chem.* **58,** 485-487.

35. M. Barber, R. S. Bordoli, G. J. Elliot, R. D. Sedgwick, A. N. Taylor, (1983) *J. Chem. Soc.*, Faraday Trans. 1, **79,** 1249-1255.

36. W. V. Ligon, S. B. Dorn, (1984) *Int. J. Mass Spectrom. Ion Proc.* **61,** 113-122.

37. L. I. Osipow, *Surface Chemistry*, R. E. Krieger Pub. Co., Huntington, New York, 1972.

38. W. V. Ligon, S. B. Dorn, (1988) *J. Am. Chem. Soc.* **110,** 6684.

39. P. J. Todd, (1988) *Proceeding of the 36th ASMS Conference on Mass Spectrometry and Allied Topics,* San Francisco, CA.

40. P. J. Todd, (1986) *Proceeding of the 34th ASMS Conference on Mass Spectrometry and Allied Topics,* Cincinnati, OH.

41. S. N. Naylor, A. F. Finders, B. W. Gibson, D. H. Williams, (1986) *J. Am. Chem. Soc.* **108,** 6359.

42. D. H. Wiliams, C. Bradley, G Bojeson, S. Santikaru, C. C. E. Taylor, (1981) *J. Am. Chem. Soc.* **103,** 5700-5704.

43. K. A. Caldwell, M. L. Gross, (1989) *Anal. Chem.* **61,** 494-496.

44. G. C. DiDonato, K. L. Busch, (1985) *Biomedical Mass Spectrometry,* **12,** 364.

45. W. V. Ligon, S. B. Dorn, (1986) *Anal. Chem.* **58,** 1889-1992.

46. W. V. Ligon, S. B. Dorn, (1985) *Anal. Chem.* **57,** 1993-1995.

47. W. V. Ligon, S. B. Dorn, (1986) *Int. J. Mass Spectrom. Ion Proc.* **68,** 337-340.

48. W. V. Ligon, S. B. Dorn, (1986) *Fresenius Z. Anal. Chem.* **325,** 626-627.

49. D. F. Barofsky, L. F. Jiang, T. Y. Yen, (1990) In "Ion Formation from Organic Solids (IFOSV);" A. Hedin, B. U. R. Sundqvist, A. Bennighoven (Eds.); Wiley, New York, p. 87.

50. Dr. E. W. Ens, Physics Department, University of Manitoba, Winnepeg, Manitoba, R3T2N2, Canada.

51. L. G. Davis, M. D. Dibner, J. F. Battey, *Basic Methods in Molecular Biology,* Elsevier Science Pub., New York, pp320-232, (1986).

52. T. Keough, (1988) *Int. J. Mass. Stctrom. Ion. Proc.* **86,** 155-168.

53. D. L. Slowikowski, K. H. Schram, (1985) *Nucleosides & Nucleotides,* **4**(3), 309-345.

54. D. L. Slowikowski, K. H. Schram, (1985) *Nucleosides & Nucleotides,* **4**(3), 347-376.

55. J. T. Watson, *Introduction to Mass Spectrometry,* 2nd Ed., Raven Press, New York, pp. 213-216, (1985).

56. Dr. J. C. Westall, Department of Chemistry, Oregon State University, Corvallis, Oregon 97331.

57. B. D. Bennet, R. A. Day, (1992) *Analytical Letters,* **25**(4), 763-778.

58. R. M. Caprioli, (1983) *Anal. Chem.* **55,** 2387-2391.

59. M. Salepour, P. Håkansson, B. U. R. Sundqvist, A. G. Craig, (1987) *Int. J. Mass Spectrom. Ion Proc.,* **77,** 173-186.

APPENDIX

Vita

James Gilbert Pavlovich was born in Anchorage, Alaska on 27 January 1962. In 1980 he entered California Polytechnic State University in San Luis Obispo, California. He received a B.S. in Chemistry in 1985. From 1985 to 1987, he was employed at Central Coast Analytical Services in San Luis Obispo as supervisor of the organics section.

The author entered graduate school at Oregon State University in January 1987. That fall he began work with Professor Douglas Barofsky. Additionally, he spent the summers of 1987 and '88 at Battelle/Pacific Northwest Laboratories in Richland, Washington as a NORCUS graduate appointee. In 1988, he received the Benedict award from the department of Chemistry at OSU. Also that year, he was awarded a Ford Foundation Predoctoral Fellowship for Minorities. He defended his Ph.D. thesis on 18 March 1993.

The author has accepted a postdoctoral research position in the Department of Environmental Sciences and Engineering at the University of North Carolina, Chapel Hill, North Carolina.